An explicit hybridizable discontinuous Galerkin method for the 3D time-domain Maxwell equations

Georges Nehmetallah, Stephane Lanteri, Stéphane Descombes

An explicit hybridizable discontinuous Galerkin method for the 3D time-domain Maxwell equations

Georges Nehmetallah, Stéphane Lanteri*, Stéphane Descombes

Université Côte d'Azur, INRIA, CNRS, LJAD, France

Abstract

We present an explicit hybridizable discontinuous Galerkin (HDG) method for numerically solving the system of three-dimensional (3D) time-domain Maxwell equations. The method is fully explicit similarly to classical so-called DGTD (Discontinuous Galerkin Time-Domain) methods that have been extensively studied during the last 15 years for the simulation of time-domain electromagnetic wave propagation. This HDGTD (Hybridizable Discontinuous Galerkin Time-Domain) method is also high-order accurate in both space and time and can be seen as a generalization of the classical DGTD scheme based on upwind fluxes. In particular, it coincides with the latter scheme for a particular choice of the stabilization parameter introduced in the definition of numerical traces in the HDG framework. It posseses a superconvergence property that allows, by means of local postprocessing, to obtain new improved approximations of the variables at any time levels. In particular, the new approximation converge with order $k + 1$ instead of k in the H^{curl}-norm for $k \geq 1$. The proposed method has been implemented for dealing with general 3D problems. We provide numerical results aiming at assessing its numerical convergence properties by considering first a model problem. Then, this HDGTD method is applied to a classical scattering problem.

Keywords: Maxwell's equations, time-domain, discontinuous Galerkin, hybridized discontinuous Galerkin

*Corresponding author
Email address:* `Stephane.Lanteri@inria.fr` (Stéphane Lanteri)

1. Motivations and objectives

1.1. Generalities about the DGTD method

During the last ten years, the DGTD method has progressively emerged as a viable alternative to well established FDTD (Finite Difference Time-Domain) [1] and FETD (Finite Element Time-Domain) [2] methods for the numerical simulation of electromagnetic wave propagation problems in the time-domain.

The DGTD method can be considered as a finite element method where the continuity constraint at an element interface is released. While it keeps almost all the advantages of the finite element method (large spectrum of applications, complex geometries, etc.), the DGTD method has other nice properties which explain the renewed interest it gains in various domains in scientific computing:

- It is naturally adapted to a high order approximation of the unknown field. Moreover, one may increase the degree of the approximation in the whole mesh as easily as for spectral methods but, with a DGTD method, this can also be done locally *i.e.* at the mesh cell level. In most cases, the approximation relies on a polynomial interpolation method but the method also offers the flexibility of applying local approximation strategies that best fit to the intrinsic features of the modeled physical phenomena.

- When the discretization in space is coupled to an explicit time integration method, the DG method leads to a block diagonal mass matrix independently of the form of the local approximation (e.g the type of polynomial interpolation). This is a striking difference with classical, continuous FETD formulations. Moreover, the mass matrix is diagonal if an orthogonal basis is chosen.

- It easily handles complex meshes. The grid may be a classical conforming finite element mesh, a non-conforming one or even a hybrid mesh made of various elements (tetrahedra, prisms, hexahedra, etc.). The DGTD method has been proven to work well with highly locally refined meshes. This property makes the DGTD method particularly well suited to the design of a hp-adaptive solution strategy (*i.e.* where the characteristic mesh size h and the interpolation degree p changes locally wherever it is needed).

- It is flexible with regards to the choice of the time stepping scheme. One may combine the discontinuous Galerkin spatial discretization with

2

any global or local explicit time integration scheme, or even implicit, provided the resulting scheme is stable.

- It is naturally adapted to parallel computing. As long as an explicit time integration scheme is used, the DGTD method is easily parallelized. Moreover, the compact nature of method is in favor of high computation to communication ratio especially when the interpolation order is increased.

As in a classical finite element framework, a discontinuous Galerkin formulation relies on a weak form of the continuous problem at hand. However, due to the discontinuity of the global approximation, this variational formulation has to be defined at the element level. Then, a degree of freedom in the design of a discontinuous Galerkin scheme stems from the approximation of the boundary integral term resulting from the application of an integration by parts to the element-wise variational form. In the spirit of finite volume methods, the approximation of this boundary integral term calls for a numerical flux function which can be based on either a centered scheme or an upwind scheme, or a blend of these two schemes.

1.2. DGTD methods for time-domain electromagnetics

In the early 2000's, DGTD methods for time-domain electromagnetics have been studied by a few groups of researchers, most of then from the applied mathematics community. One of the most significant contributions is due to Hesthaven and Warburton [3] in the form of a high order nodal DGTD method formulated on unstructured simplicial meshes. The proposed formulation is based on an upwind numerical flux, nodal basis expansions on a triangle (2D case) and a tetrahedron (3D case) and a Runge-Kutta time stepping scheme. In [4], Kakbian *et al.* describe a rather similar approach. More precisely, the authors develop a parallel, unstructured, high order DGTD method based on simple monomial polynomials for spatial discretization, an upwind numerical flux and a fourth-order Runge-Kutta scheme for time marching. The method has been implemented with hexahedral and tetrahedral meshes. A high order DGTD method based on a strong stability preserving Runge-Kutta time scheme has been studied by Chen *et al.* [5]. The authors also present post-processing techniques that can double the convergence order. A locally divergence-free DGTD method is formulated and studied by Cockburn *et al.* in [6]. In the same period, a high order nodal DGTD method formulated on unstructured simplicial meshes has also been proposed by Fezoui *et al.* [7]. However, contrary to the DGTD methods discussed in [3] and [4], the method proposed in [7] is non-dissipative thanks to a combination of a

centered numerical flux with a second-order leap-frog time stepping scheme. The DGTD method has then been progressively considered and extended to increasingly more complex modeling situations by groups of researchers in the applied electromagnetics and electrical engineering communities for a wide variety of applications related to aeronautics, defense, semiconductor device fabrication, etc. [8]-[9]-[10]-[11]-[12]-[13]-[14] to cite a few. More recently, the method has also been adopted and further developed by researchers in the nano-optics domain [15]-[16]-[17]-[18]. A full review of the nowadays numerous applications of DGTD methods would certainly require more than a simple paragraph. Also worth to note, the DGTD method has been implement in commercial software such HFSS-TD (the time-domain version of the well-known HFSS software used for antenna design) [19].

1.3. Explicit versus implicit DGTD methods

From the above discussion, it is clear that the DGTD method is nowadays a very popular numerical method in the computational electromagnetics community. The works mentioned so far are mostly concerned with time explicit DGTD methods relying on the use of a single global time step computed so as to ensure stability of the simulation. It is however well known that when combined with an explicit time integration method and in the presence of an unstructured locally refine mesh, a high order DGTD method suffers from a severe time step size restriction. A possible alternative to overcome this limitation is to use smaller time steps, given by a local stability criterion, precisely where the smallest elements are located. The local character of a DG formulation is a very attractive feature for the development of explicit local time stepping schemes. Such techniques have been developed for the second order wave equation discretized in space by a DG method [20]-[21]. In [22], a second order symplectic local time stepping DGTD method is proposed for Maxwell's equations in a non-conducting medium, based on the Störmer-Verlet method. Grote and Mitkova derived local time-stepping methods of arbitrarily high accuracy for Maxwell's equations from the standard leap-frog scheme [23]. In [24], Taube *et al.* also proposed an arbitrary high order local time-stepping method based on ADER DG approach for Maxwell's equation. An alternative approach that has been considered in [25]-[26] is to use a hybrid explicit-implicit (or locally implicit) time integration strategy. Such a strategy relies on a component splitting deduced from a partitioning of the mesh cells in two sets respectively gathering coarse and fine elements. In these works, a second order explicit leap-frog scheme is combined with a second order implicit Crank-Nicolson scheme in the framework of a non-dissipative (centered flux based) DG discretization in space. At each time step, a large

4

linear system must be solved whose structure is partly diagonal (for those rows of the system associated to the explicit unknowns) and partly sparse (for those rows of the system associated to the implicit unknowns). The computational efficiency of this locally implicit DGTD method depends on the size of the set of fine elements that directly influences the size of the sparse part of the matrix system. Therefore, an approach for reducing the size of the subsystem of globally coupled (i.e. implicit) unknowns is worth considering if one wants to solver very large-scale problems.

A particularly appealing solution in this context is given by the concept of hybridizable discontinuous Galerkin (HDG) method. The HDG method has been first introduced by Cockbrun *et al.* in [27] for a model elliptic problem and has been subsequently developed for a variety of PDE systems in continuum mechanics [28]. The essential ingredients of a HDG method are

1. a local Galerkin projection of the underlying system of PDEs at the element level onto spaces of polynomials to parametrize the numerical solution in terms of the numerical trace,
2. a judicious choice of the numerical flux to provide stability and consistency,
3. a global jump condition that enforces the continuity of the numerical flux to arrive at a global weak formulation in terms of the numerical trace.

HDG methods are fully implicit, high-order accurate and endowed with several unique features which distinguish themselves from other discontinuous Galerkin methods. Most importantly, they reduce the globally coupled unknowns to the approximate trace of the solution on element boundaries, thereby leading to a significant reduction in the degrees of freedom. HDG methods for the system of time-harmonic Maxwell equations have been proposed in [29]-[30]-[31].

1.4. Objectives of this work

As mentioned previously, HDG methods are essentially fully implicit. Our ultimate goal is to devise a high order hybrid explicit-implicit HDG method. A preliminary step considered in this work is therefore to elaborate on the principles of a fully explicit HDG formulation. It happens that fully explicit HDG methods have been studied recently for acoustic wave equation by Kronbichler *al.* [32] and Stanglmeier *al.* [33]. The work reported in [32] is in fact a comparison of implicit and explicit HDG formulations. In the explicit HDG scheme, the trace of the acoustic pressure on a face is computed from the solution of the two elements adjacent to the face at the

old time step. The adopted time integration schemes are diagonally implicit and explicit Runge-Kutta schemes. The conclusion of this study is that for the considered acoustic wave propagation problems, the computing time per time step is much lower for the explicit scheme, which is two orders of magnitude more efficient than the implicit scheme despite the stability restriction on the time step of the explicit scheme. In [33] the authors present a fully explicit, high order accurate in both space and time HDG method. The method coincides with the classical upwind flux-based DG method for a particular choice of the stabilization parameter in the HDG numerical traces. Time integration is obtained by a strong stability preserving Runge-Kutta scheme. This HDG method provides an optimal convergence rate for the solution and its gradient and is amenable to local post-processing to obtain a superconvergence property with a rate $k + 2$ if k, $k \geq 1$, is the interpolation order in the L^2-norm, depending on the form of the numerical fluxes.

In this paper we propose a fully explicit high order accurate HDG method for the solution of the system of time-domain Maxwell equations. We adopt a low storage Runge-Kutta scheme [34] for the time integration of the semi-discrete HDG equations. It also provides an optimal convergence rate for the solution and is amenable to local post-processing to obtain a superconvergence property with a rate $k + 1$ if $k \geq 1$ is the interpolation order in the H^{curl}-norm instead of k. As in [33], we show that for a particular choice of the stabilization parameter in the definition of the HDG numerical traces, we recover the classical upwind flux-based DG method [3]. This work is a first step towards the construction of a hybrid explicit-implicit HDG method for time-domain electromagnetics.

2. Problem statement and notations

2.1. Initial and boundary value prolem

We consider the system of 3D time-domain Maxwell's equations on a bounded polyhedral domain $\Omega \subset \mathbb{R}^3$

$$\begin{cases} \varepsilon \partial_t \mathbf{E} - \mathbf{curl}\,\mathbf{H} = -\mathbf{J}, \ \text{in } \Omega \times [0, T], \\ \mu \partial_t \mathbf{H} + \mathbf{curl}\,\mathbf{E} = 0, \ \text{in } \Omega \times [0, T], \end{cases} \tag{1}$$

where the symbol ∂_t denotes a time derivate, $\mathbf{J}$ the current density, T a final time, $\mathbf{E}(\mathbf{x}, t)$ and $\mathbf{H}(\mathbf{x}, t)$ are the electric and magnetic fields. The relative dielectric permittivity ε and the relative magnetic permeability μ are varying in space, time-invariant and both positive functions. The boundary of Ω is

defined as $\partial \Omega = \Gamma_m \cup \Gamma_a$ with $\Gamma_m \cap \Gamma_a = \emptyset$. The boundary conditions are choosen as

$$
\begin{cases}
\mathbf{n} \times \mathbf{E} = 0, \text{ on } \Gamma_m \times [0, T], \\
\mathbf{n} \times \mathbf{E} + \mathbf{n} \times (\mathbf{n} \times \mathbf{H}) = \mathbf{n} \times \mathbf{E}^{\text{inc}} + \mathbf{n} \times (\mathbf{n} \times \mathbf{H}^{\text{inc}}) \\
\qquad\qquad\qquad = \mathbf{g}^{\text{inc}}, \text{ on } \Gamma_a \times [0, T].
\end{cases}
\tag{2}
$$

Here $\mathbf{n}$ denotes the unit outward normal to $\partial \Omega$ and $(\mathbf{E}^{\text{inc}}, \mathbf{H}^{\text{inc}})$ a given incident field. The first boundary condition is often referred as a metallic boundary condition and is applied on a perfectly conducting surface. The second relation is an absorbing boundary condition and takes here the form of the Silver-Müller condition. It is applied on a surface corresponding to an artificial truncature of a theoretically unbounded propagation domain. Finally, the system is supplemented with inital conditions: $\mathbf{E}_0(\mathbf{x}) = \mathbf{E}(\mathbf{x}, 0)$ and $\mathbf{H}_0(\mathbf{x}) = \mathbf{H}(\mathbf{x}, 0)$. For sake of simplicity, we omit the volume source term $\mathbf{J}$ in what follows.

2.2. Notations and approximation spaces

We consider a partition $\mathcal{T}_h$ of $\Omega \subset \mathbb{R}^3$ into a set of tetraedra. Each non-empty intersection of two elements K^+ and K^- is called an interface. We denote by $\mathcal{F}_h^I$ the union of all interior interfaces of $\mathcal{T}_h$, by $\mathcal{F}_h^B$ the union of all boundary interfaces of $\mathcal{T}_h$, and $\mathcal{F}_h = \mathcal{F}_h^I \cup \mathcal{F}_h^B$. Note that $\partial \mathcal{T}_h$ represents all the interfaces ∂K for all $K \in \mathcal{T}_h$. As a result, an interior interface shared by two elements appears twice in $\partial \mathcal{T}_h$, unlike in $\mathcal{F}_h$ where this interface is evaluated once. For an interface $F \in \mathcal{F}_h^I$, $F = \overline{K}^+ \cap \overline{K}^-$, let $\mathbf{v}^\pm$ be the traces of $\mathbf{v}$ on F from the interior of $K^\pm$. On this interior face, we define mean values $\{\cdot\}$ and jumps $[\![\cdot]\!]$ as

$$
\begin{cases}
\{\mathbf{v}\}_F = \dfrac{1}{2}(\mathbf{v}^+ + \mathbf{v}^-), \\
[\![\mathbf{v}]\!]_F = \mathbf{n}^+ \times \mathbf{v}^+ + \mathbf{n}^- \times \mathbf{v}^-,
\end{cases}
$$

where the unit outward normal vector to K is denoted by $\mathbf{n}^\pm$. For the boundary faces these expressions are modified as

$$
\begin{cases}
\{\mathbf{v}\}_F = \mathbf{v}^+, \\
[\![\mathbf{v}]\!]_F = \mathbf{n}^+ \times \mathbf{v}^+.
\end{cases}
$$

since we assume $\mathbf{v}$ is single-valued on the boundaries. In the following, we introduce the discontinuous finite element spaces and some basic operations

7

on these spaces for later use. Let $\mathbb{P}_{p_K}(K)$ denotes the space of polynomial functions of degree at most p_K on the element $K \in \mathcal{T}_h$. The discontinuous finite element space is as usual defined as

$$\mathbf{V}_h = \left\{ \mathbf{v} \in \left[L^2(\Omega) \right]^3 \text{ such that } \mathbf{v}|_K \in \left[\mathbb{P}_{p_K}(K) \right]^3, \quad \forall K \in \mathcal{T}_h \right\}, \quad (3)$$

where $L^2(\Omega)$ is the space of square integrable functions on the domain Ω. The functions in $\mathbf{V}_h$ are continuous inside each element and discontinuous across the interfaces between elements. In addition, we introduce a traced finite element space $\mathbf{M}_h$

$$
\begin{aligned}
\mathbf{M}_h = \Big\{ &\boldsymbol{\eta} \in \left[L^2(\mathcal{F}_h) \right]^3 \text{ such that } \boldsymbol{\eta}|_F \in \left[\mathbb{P}_{p_F}(F) \right]^3 \\
&\text{and } (\boldsymbol{\eta} \cdot \mathbf{n})|_F = 0, \quad \forall F \in \mathcal{F}_h \Big\}.
\end{aligned}
\quad (4)
$$

Let us define D as a domain in $\mathbb{R}^3$. For two vectorial functions $\mathbf{u}$ and $\mathbf{v}$ in $\left[L^2(D) \right]^3$, we denote $(\mathbf{u}, \mathbf{v})_D = \int_D \mathbf{u} \cdot \mathbf{v} \, \mathrm{d}\mathbf{x}$, and we denote $< \mathbf{u}, \mathbf{v} >_F = \int_F \mathbf{u} \cdot \mathbf{v} \, \mathrm{d}s$ if F is a two-dimensional face. Accordingly, for the mesh $\mathcal{T}_h$ we have

$$(\cdot, \cdot)_{\mathcal{T}_h} = \sum_{K \in \mathcal{T}_h} (\cdot, \cdot)_K, \qquad \langle \cdot, \cdot \rangle_{\partial \mathcal{T}_h} = \sum_{K \in \mathcal{T}_h} \langle \cdot, \cdot \rangle_{\partial K},$$

$$\langle \cdot, \cdot \rangle_{\mathcal{F}_h} = \sum_{F \in \mathcal{F}_h} \langle \cdot, \cdot \rangle_F, \qquad \langle \cdot, \cdot \rangle_{\Gamma_a} = \sum_{F \in \mathcal{F}_h \cap \Gamma_a} \langle \cdot, \cdot \rangle_F.$$

We set $\mathbf{v}^t = -\mathbf{n} \times (\mathbf{n} \times \mathbf{v})$, $\quad \mathbf{v}^n = \mathbf{n} (\mathbf{n} \cdot \mathbf{v})$ where $\mathbf{v}^t$ and $\mathbf{v}^n$ are the tangential and normal components of $\mathbf{v}$ such as $\mathbf{v} = \mathbf{v}^t + \mathbf{v}^n$.

3. Principles and formulation of the HDG method

3.1. Global formulation

Following the classical DG approach, approximate solutions $(\mathbf{E}_h, \mathbf{H}_h)$, for all $t \in [0, T]$, are sought in the space $\mathbf{V}_h \times \mathbf{V}_h$ satisfying for all K in $\mathcal{T}_h$

$$
\begin{cases}
(\varepsilon \partial_t \mathbf{E}_h, \mathbf{v})_K - (\mathbf{curl}\, \mathbf{H}_h, \mathbf{v})_K = 0, \ \forall \mathbf{v} \in \mathbf{V}_h, \\
(\mu \partial_t \mathbf{H}_h, \mathbf{v})_K + (\mathbf{curl}\, \mathbf{E}_h, \mathbf{v})_K = 0, \ \forall \mathbf{v} \in \mathbf{V}_h.
\end{cases}
\quad (5)
$$

Applying Green's formula, on both equations of (5) introduces boundary terms which are replaced by numerical traces $\hat{\mathbf{E}}_h$ and $\hat{\mathbf{H}}_h$ in order to ensure

the connection between element-wise solutions and global consistency of the discretization. This leads to the formulation for all $t \in [0, T]$

$$
\begin{cases}
(\varepsilon \partial_t \mathbf{E}_h, \mathbf{v})_K - (\mathbf{H}_h, \mathbf{curl}\, \mathbf{v})_K + \left\langle \hat{\mathbf{H}}_h, \mathbf{n} \times \mathbf{v} \right\rangle_{\partial K} = 0, \ \forall \mathbf{v} \in \mathbf{V}_h, \\
(\mu \partial_t \mathbf{H}_h, \mathbf{v})_K + (\mathbf{E}_h, \mathbf{curl}\, \mathbf{v})_K - \left\langle \hat{\mathbf{E}}_h, \mathbf{n} \times \mathbf{v} \right\rangle_{\partial K} = 0, \ \forall \mathbf{v} \in \mathbf{V}_h.
\end{cases}
\tag{6}
$$

It is straightforward to verify that $\mathbf{n} \times \mathbf{v} = \mathbf{n} \times \mathbf{v}^t$ and $< \mathbf{H}, \mathbf{n} \times \mathbf{v} > = - < \mathbf{n} \times \mathbf{H}, \mathbf{v} >$. Therefore, using numerical traces defined in terms of the tangential components $\hat{\mathbf{H}}_h^t$ and $\hat{\mathbf{E}}_h^t$, we can rewrite (6) as

$$
\begin{cases}
(\varepsilon \partial_t \mathbf{E}_h, \mathbf{v})_K - (\mathbf{H}_h, \mathbf{curl}\, \mathbf{v})_K + \left\langle \hat{\mathbf{H}}_h^t, \mathbf{n} \times \mathbf{v} \right\rangle_{\partial K} = 0, \ \forall \mathbf{v} \in \mathbf{V}_h, \\
(\mu \partial_t \mathbf{H}_h, \mathbf{v})_K + (\mathbf{E}_h, \mathbf{curl}\, \mathbf{v})_K - \left\langle \hat{\mathbf{E}}_h^t, \mathbf{n} \times \mathbf{v} \right\rangle_{\partial K} = 0, \ \forall \mathbf{v} \in \mathbf{V}_h.
\end{cases}
\tag{7}
$$

The hybrid variable $\mathbf{\Lambda}_h$ introduced in the setting of a HDG method [27] is here defined for all the interfaces of $\mathcal{F}_h$ as

$$
\mathbf{\Lambda}_h := \hat{\mathbf{H}}_h^t, \quad \forall F \in \mathcal{F}_h.
\tag{8}
$$

We want to determine the fields $\hat{\mathbf{H}}_h^t$ and $\hat{\mathbf{E}}_h^t$ in each element K of $\mathcal{T}_h$ by solving system (7) and assuming that $\mathbf{\Lambda}_h$ is known on all the faces of an element K. We consider a numerical trace $\hat{\mathbf{E}}_h^t$ for all K given by

$$
\hat{\mathbf{E}}_h^t = \mathbf{E}_h^t + \tau_K \mathbf{n} \times (\mathbf{\Lambda}_h - \mathbf{H}_h^t) \text{ on } \partial K,
\tag{9}
$$

where τ_K is a local stabilization parameter which is assumed to be strictly positive. We recall that $\mathbf{n} \times \mathbf{H}_h^t = \mathbf{n} \times \mathbf{H}_h$. Note that the definitions of the hybrid variable (8) and numerical trace (9) are exactly those adopted in the context of the formulation of HDG methods for the 3D time-harmonic Maxwell equations [29]-[31].

Remark 1. In a classical DG method the traces of the local fields $\mathbf{E}_h$ and $\mathbf{H}_h$ between neighboring elements are defined as

$$
\hat{\mathbf{E}}_h = \{\mathbf{E}_h\} + \alpha_H [\![\mathbf{H}_h]\!] \text{ and } \hat{\mathbf{H}}_h = \{\mathbf{H}_h\} + \alpha_E [\![\mathbf{E}_h]\!],
$$

where α_H and α_E are positive penalty parameters.

Remark 2. Following the HDG approach, when the hybrid variable $\mathbf{\Lambda}_h$ is known for all the faces of the element K, the electromagnetic field can be determined by solving the local system (7) using (8) and (9).

For the sake of simplicity, we denote by $\mathbf{g}^{\mathrm{inc}}$ the L^2 projection of $\mathbf{g}^{\mathrm{inc}}$ on $\mathbf{M}_h$. Summing the contributions of (7) over all the elements and enforcing the continuity of the tangential component of $\hat{\mathbf{E}}_h$, we can formulate a problem which is to find $(\mathbf{E}_h, \mathbf{H}_h, \boldsymbol{\Lambda}_h) \in \mathbf{V}_h \times \mathbf{V}_h \times \mathbf{M}_h$ such that for all $t \in [0, T]$

$$
\begin{aligned}
(\varepsilon \partial_t \mathbf{E}_h, \mathbf{v})_{\mathcal{T}_h} - (\mathbf{H}_h, \mathbf{curl}\,\mathbf{v})_{\mathcal{T}_h} + \langle \boldsymbol{\Lambda}_h, \mathbf{n} \times \mathbf{v} \rangle_{\partial \mathcal{T}_h} &= 0, \ \forall \mathbf{v} \in \mathbf{V}_h, \\
(\mu \partial_t \mathbf{H}_h, \mathbf{v})_{\mathcal{T}_h} + (\mathbf{E}_h, \mathbf{curl}\,\mathbf{v})_{\mathcal{T}_h} - \left\langle \hat{\mathbf{E}}_h^t, \mathbf{n} \times \mathbf{v} \right\rangle_{\partial \mathcal{T}_h} &= 0, \ \forall \mathbf{v} \in \mathbf{V}_h, \\
\left\langle [\![\hat{\mathbf{E}}_h]\!], \boldsymbol{\eta} \right\rangle_{\mathcal{F}_h} - \langle \boldsymbol{\Lambda}_h, \boldsymbol{\eta} \rangle_{\Gamma_a} - \left\langle \mathbf{g}^{\mathrm{inc}}, \boldsymbol{\eta} \right\rangle_{\Gamma_a} &= 0, \ \forall \boldsymbol{\eta} \in \mathbf{M}_h,
\end{aligned} \tag{10}
$$

where the last equation is called the conservativity condition with which we ask the tangential component of $\hat{\mathbf{E}}_h$ to be weakly continuous across any interface between two neighboring elements.

The main principles of the HDG method can be summarized as

1. The DoFs (Degrees of Freedoms) of the hybrid variable are determined by solving a global linear system (from the discretization of the conservation condition) supported by the interfaces of $\mathcal{F}_h$;
2. The DoFs of the electromagnetic field in each element are evaluated by solving local linear systems, more exactly for the DoFs of $(\mathbf{E}_h, \mathbf{H}_h)$ in the considered element.

3.2. Reformulation with numerical fluxes

From the third equation of (10) we have

$$
\left\langle [\![\hat{\mathbf{E}}_h^t]\!], \boldsymbol{\eta} \right\rangle_{\mathcal{F}_h^I} = 0 \quad \forall \boldsymbol{\eta} \in \mathbf{M}_h \cap \{ \boldsymbol{\eta} = 0 \quad \text{on}\, (\mathcal{F}_h \cap \Gamma_m) \cup (\mathcal{F}_h \cap \Gamma_a) \}.
$$

Now, let us prove that the function

$$
\boldsymbol{\eta}_1 = \begin{cases} [\![\hat{\mathbf{E}}_h^t]\!] & \text{on} \quad \mathcal{F}_h^I \\ 0 & \text{on} \quad (\mathcal{F}_h \cap \Gamma_m) \cup (\mathcal{F}_h \cap \Gamma_a) \end{cases}
$$

belongs to the space $\mathbf{M}_h \cap \{ \boldsymbol{\eta} = 0 \,\text{on}\, (\mathcal{F}_h \cap \Gamma_m) \cup (\mathcal{F}_h \cap \Gamma_a) \}$,

First it is clear that $\mathbf{n} \cdot \boldsymbol{\eta}_1|_F = 0$ for all $F \in \mathcal{F}_h^I$ and we have

$$
\begin{aligned}
[\![\hat{\mathbf{E}}_h^t]\!] &= \mathbf{n}^+ \times \hat{\mathbf{E}}_h^{t,+} + \mathbf{n}^- \times \hat{\mathbf{E}}_h^{t,-} \\
&= \mathbf{n}^+ \times \mathbf{E}_{h|K^+}^+ + \tau_{K^+} \mathbf{n}^+ \times \mathbf{n}^+ \times (\boldsymbol{\Lambda}_h - \mathbf{H}_{h|K^+}^+) \\
&\quad + \mathbf{n}^- \times \mathbf{E}_{h|K^-}^- + \tau_{K^-} \mathbf{n}^- \times \mathbf{n}^- \times (\boldsymbol{\Lambda}_h - \mathbf{H}_{h|K^-}^-).
\end{aligned}
$$

Since K is a bounded domain and $\mathbf{n}$ is constant on every face we have that $\left(\mathbf{n} \times \mathbf{E}_{h|K}\right)_{|F}$ and $\left(\mathbf{n} \times \mathbf{H}_{h|K}\right)_{|F}$ are bounded polynoms in $[\mathbb{P}_{p_F}(F)]^3$ $\forall F \in \partial K$, which implies that $\boldsymbol{\eta}_1 \in \left[L^2\left(\mathcal{F}_h\right)\right]^3$ and $\boldsymbol{\eta}_1|_F \in [\mathbb{P}_{p_F}(F)]^3$ $\forall F \in \partial K$. We obtain $\left\langle [\![\hat{\mathbf{E}}_h^t]\!], \boldsymbol{\eta}_1 \right\rangle_{\mathcal{F}_h^I} = ||[\![\hat{\mathbf{E}}_h^t]\!]||^2 = 0$, which is equivalent to $[\![\hat{\mathbf{E}}_h^t]\!]_{\mathcal{F}_h^I} = 0$. From (9), we have

$$[\![\mathbf{E}_h^t + \tau \mathbf{n} \times (\mathbf{\Lambda}_h - \mathbf{H}_h^t)]\!]_{\mathcal{F}_h^I} = 0,$$

by expanding we obtain

$$[\![\mathbf{E}_h^t]\!]_F - (\tau_{K+} + \tau_{K-})\mathbf{\Lambda}_h + \tau_{K+}\mathbf{H}_h^{t,+} + \tau_{K-}\mathbf{H}_h^{t,-} = 0 \quad \forall F \in \mathcal{F}_h^I,$$

yielding

$$\mathbf{\Lambda}_h = \frac{1}{\tau_{K+} + \tau_{K-}} \left([\![\mathbf{E}_h^t]\!]_F + \tau_{K+}\mathbf{H}_h^{t,+} + \tau_{K-}\mathbf{H}_h^{t,-}\right) \quad \forall F \in \mathcal{F}_h^I. \qquad (11)$$

Proceeding similarly for an absorbing boundary face and for a metalic boundary face, the conservativity condition writes $\left\langle \mathbf{n} \times \hat{\mathbf{E}}_h^t - \mathbf{\Lambda}_h - \mathbf{g}^{\text{inc}}, \boldsymbol{\eta} \right\rangle_{\Gamma_a} = 0$ and $\left\langle \mathbf{n} \times \hat{\mathbf{E}}_h^t, \boldsymbol{\eta} \right\rangle_{\Gamma_m} = 0$. In particular, for an absorbing boundary face

$$\mathbf{n} \times \hat{\mathbf{E}}_h^t - \mathbf{\Lambda}_h - \mathbf{g}^{\text{inc}} = 0 \quad \text{on } \Gamma_a,$$

and by (9) we have

$$\mathbf{n} \times \mathbf{E}_h^t - (\tau_K + 1)\mathbf{\Lambda}_h + \tau_K \mathbf{H}_h^t - \mathbf{g}^{\text{inc}} = 0 \quad \text{on } \Gamma_a.$$

Proceeding similarly for the metalic boundary and summarizing, we obtain

$$\mathbf{\Lambda}_h = \begin{cases} \dfrac{1}{\tau_{K+} + \tau_{K-}} \left(2\left\{\tau_K \mathbf{H}_h^t\right\}_F + [\![\mathbf{E}_h^t]\!]_F\right), & \text{if } F \in \mathcal{F}_h^I, \\[2ex] \dfrac{1}{\tau_K}\mathbf{n} \times \mathbf{E}_h^t + \mathbf{H}_h^t, & \text{if } F \in \mathcal{F}_h \cap \Gamma_m, \\[2ex] \dfrac{1}{\tau_K + 1} \left(\tau_K \mathbf{H}_h^t + \mathbf{n} \times \mathbf{E}_h^t - \mathbf{g}^{\text{inc}}\right). & \text{if } F \in \mathcal{F}_h \cap \Gamma_a. \end{cases} \qquad (12)$$

By replacing (12) in (9) we obtain $\hat{\mathbf{E}}_h^t = \hat{\mathbf{E}}_h^{t,+} = \hat{\mathbf{E}}_h^{t,-}$ with

$$\hat{\mathbf{E}}_h^t = \begin{cases} \dfrac{\tau_{K+}\tau_{K-}}{\tau_{K+} + \tau_{K-}} \left(2\left\{\dfrac{1}{\tau_K}\mathbf{E}_h^t\right\}_F - [\![\mathbf{H}_h^t]\!]_F\right), & \text{if } F \in \mathcal{F}_h^I, \\[2ex] 0, & \text{if } F \in \mathcal{F}_h \cap \Gamma_m, \\[2ex] \dfrac{1}{\tau_K + 1} \left(\mathbf{E}_h^t - \tau_K \mathbf{n} \times \mathbf{H}_h^t - \tau_K \mathbf{n} \times \mathbf{g}^{\text{inc}}\right). & \text{if } F \in \mathcal{F}_h \cap \Gamma_a. \end{cases} \qquad (13)$$

11

Thus, the numerical traces (8) and (9) have been reformulated from the conservativity condition. This means that the conservativity condition is now included in the new formulation of the numerical fluxes and can be omitted in the global system of equations. Hence, the local system (6) takes the form of a classical DG formulation, for all $\mathbf{v} \in \mathbf{V}_h$

$$
\begin{cases}
(\varepsilon \partial_t \mathbf{E}_h, \mathbf{v})_K - (\mathbf{H}_h, \mathbf{curl}\,\mathbf{v})_K + \left\langle \hat{\mathbf{H}}_h^t, \mathbf{n} \times \mathbf{v} \right\rangle_{\partial K} = 0, \\
(\mu \partial_t \mathbf{H}_h, \mathbf{v})_K + (\mathbf{E}_h, \mathbf{curl}\,\mathbf{v})_K - \left\langle \hat{\mathbf{E}}_h^t, \mathbf{n} \times \mathbf{v} \right\rangle_{\partial K} = 0.
\end{cases}
\tag{14}
$$

where the numerical fluxes are defined by (12) and (13).

Remark 3. Let $Y_K = \sqrt{\dfrac{\varepsilon_K}{\mu_K}}$ be the local admittance associated to cell K and $Z_K = 1/Y_K$ the corresponding local impedance. If we set $\tau_K = Z_K$ in (12) and $1/\tau_K = Y_K$ in (13), the obtained numerical traces coincide with those adopted in the classical upwind flux DGTD method [3].

3.3. Stability and conservation properties

3.3.1. Formulation

After summing the two equations of the local formulation (14) we obtain $\forall \boldsymbol{v}_h' \in \mathbb{V}_h = \mathbf{V}_h \times \mathbf{V}_h$

$$
\left(\lambda \partial_t \boldsymbol{v}_h, \boldsymbol{v}_h'\right)_K = \left(\boldsymbol{v}_h, \zeta_K(\boldsymbol{v}_h')\right)_K - \left\langle \mathbf{F}_{K,h}^\tau(\boldsymbol{v}_h), \boldsymbol{v}_h' \right\rangle_{\partial K},
\tag{15}
$$

where $\boldsymbol{v}_h = \begin{pmatrix} \mathbf{H}_h \\ \mathbf{E}_h \end{pmatrix}$, $\lambda = \mathrm{diag}(\mu, \varepsilon)$ and for all $K \in \mathcal{T}_h$, for all $\boldsymbol{v} \in \mathbb{V}_h$

$$
\zeta_K(\boldsymbol{v}) = \begin{pmatrix} \mathbf{curl}\left(\boldsymbol{v}_{2/K}\right) \\ -\mathbf{curl}\left(\boldsymbol{v}_{1/K}\right) \end{pmatrix}.
$$

Assuming τ is constant in $\mathcal{T}_h$ and $g^{inc} = 0$, the numerical flux $\mathbf{F}_{K,h}^\tau$ is defined on ∂K by

$$
\mathbf{F}_{K,h}^\tau(\boldsymbol{v})_{|\partial K \cap \mathcal{F}_h^I} = \begin{pmatrix} \dfrac{\tau}{2}\left(\dfrac{2}{\tau}\mathbf{n} \times \{\boldsymbol{v}_2\} - \mathbf{n} \times [\![\boldsymbol{v}_1]\!]\right) \\ -\dfrac{1}{2\tau}\left(2\tau \mathbf{n} \times \{\boldsymbol{v}_1\} + \mathbf{n} \times [\![\boldsymbol{v}_2]\!]\right) \end{pmatrix},
$$

and

$$
\mathbf{F}_{K,h}^\tau(\boldsymbol{v})_{|\partial K \cap \Gamma_m} = \begin{pmatrix} 0 \\ \dfrac{1}{\tau}\left(\mathbf{n} \times \mathbf{n} \times \boldsymbol{v}_2\right) + \mathbf{n} \times \boldsymbol{v}_1 \end{pmatrix},
$$

$$\mathbf{F}^{\tau}_{K,h}(\boldsymbol{v})_{|\partial K \cap \Gamma_a} = \begin{pmatrix} -\dfrac{1}{\tau+1}\left(\mathbf{n}\times\boldsymbol{v}_2\right) + \dfrac{\tau}{\tau+1}\left(\mathbf{n}\times\mathbf{n}\times\boldsymbol{v}_1\right) \\ \dfrac{\tau}{\tau+1}\left(\mathbf{n}\times\boldsymbol{v}_1\right) + \dfrac{1}{\tau+1}\left(\mathbf{n}\times\mathbf{n}\times\boldsymbol{v}_2\right) \end{pmatrix}.$$

For the global weak formulation we define for all $\boldsymbol{v}\in\mathbb{V}_h$

$$\zeta_h\left(\boldsymbol{v}\right) = \begin{pmatrix} \mathbf{curl}_h\left(\boldsymbol{v}_2\right) \\ -\mathbf{curl}_h\left(\boldsymbol{v}_1\right) \end{pmatrix},$$

with $\mathbf{curl}_h$ is the piecewise curl operator defined on each K and for all $\mathbf{b}_h$ as $(\mathbf{curl}_h\left(\mathbf{b}_h\right))_{|K} = \mathbf{curl}\left(\mathbf{b}_{h|K}\right)$. The bilinear forms m, a, b_τ defined on $\mathbb{V}_h\times\mathbb{V}_h$ such that, for all $(\boldsymbol{v},\boldsymbol{v}')\in\mathbb{V}_h\times\mathbb{V}_h$

$$
\begin{cases}
m(\boldsymbol{v},\boldsymbol{v}') = (\boldsymbol{v},\boldsymbol{v}')_\lambda = (\lambda\boldsymbol{v},\boldsymbol{v}')_{\mathcal{T}_h} \\
a(\boldsymbol{v},\boldsymbol{v}') = (\boldsymbol{v},\zeta_h(\boldsymbol{v}'))_{\mathcal{T}_h} \\
b_\tau(\boldsymbol{v},\boldsymbol{v}') = \left\langle\{\boldsymbol{v}_2\},[\![\boldsymbol{v}'_1]\!]\right\rangle_{\mathcal{F}^I_h} - \dfrac{\tau}{2}\left\langle[\![\boldsymbol{v}_1]\!],[\![\boldsymbol{v}'_1]\!]\right\rangle_{\mathcal{F}^I_h} - \left\langle\{\boldsymbol{v}_1\},[\![\boldsymbol{v}'_2]\!]\right\rangle_{\mathcal{F}^I_h} \\
\quad -\dfrac{1}{2\tau}\left\langle[\![\boldsymbol{v}_2]\!],[\![\boldsymbol{v}'_2]\!]\right\rangle_{\mathcal{F}^I_h} - \dfrac{1}{\tau}\displaystyle\int_{\Gamma_m}\left(\mathbf{n}\times\boldsymbol{v}_2\right)\cdot\left(\mathbf{n}\times\boldsymbol{v}'_2\right) \\
\quad +\displaystyle\int_{\Gamma_m}\left(\mathbf{n}\times\boldsymbol{v}_1\right)\cdot\boldsymbol{v}'_2 - \dfrac{1}{\tau+1}\displaystyle\int_{\Gamma_a}\left(\mathbf{n}\times\boldsymbol{v}_2\right)\cdot\boldsymbol{v}'_1 \\
\quad -\dfrac{\tau}{\tau+1}\displaystyle\int_{\Gamma_a}\left(\mathbf{n}\times\boldsymbol{v}_1\right)\cdot\left(\mathbf{n}\times\boldsymbol{v}'_1\right) + \dfrac{\tau}{\tau+1}\displaystyle\int_{\Gamma_a}\left(\mathbf{n}\times\boldsymbol{v}_1\right)\cdot\boldsymbol{v}'_2 \\
\quad -\dfrac{1}{\tau+1}\displaystyle\int_{\Gamma_a}\left(\mathbf{n}\times\boldsymbol{v}_2\right)\cdot\left(\mathbf{n}\times\boldsymbol{v}'_2\right)
\end{cases}
\tag{16}
$$

The global formulation of the semi-discrete HDG scheme writes as

$$m(\partial_t\boldsymbol{v}_h,\boldsymbol{v}'_h) = a(\boldsymbol{v}_h,\boldsymbol{v}'_h) + b_\tau(\boldsymbol{v}_h,\boldsymbol{v}'_h). \tag{17}$$

3.3.2. Semi-discrete stability
Definition
The energy function is defined on $[0,T]$ by

$$\mathcal{E}_h(t) = \frac{1}{2}\left(\varepsilon||\mathbf{E}_h(t)||^2 + \mu||\mathbf{H}_h(t)||^2\right) = \frac{1}{2}m(\boldsymbol{v}_h,\boldsymbol{v}_h) = \frac{1}{2}||\boldsymbol{v}_h||^2_\lambda.$$

Proposition
$\forall\tau>0$ the energy function $\mathcal{E}_h(t)$ decreases in time and $\mathcal{E}_h(t) < \mathcal{E}_h(0)$ for all $t>0$.

Proof

By the formula $\partial_t ||\mathbf{v}||^2 = 2 (\partial_t \mathbf{v}, \mathbf{v})$ we have $\partial_t \mathcal{E}_h(t) = m(\partial_t \boldsymbol{v}_h, \boldsymbol{v}_h)$ and, using the formula $\displaystyle\int_K \mathbf{curl}\, \mathbf{u} \cdot \mathbf{v} = \int_K \mathbf{curl}\, \mathbf{v} \cdot \mathbf{u} + \int_{\partial K} (\mathbf{n} \times \mathbf{u}) \cdot \mathbf{v}$,
we deduce from (17) that

$$\partial_t \mathcal{E}_h(t) = a(\boldsymbol{v}_h, \boldsymbol{v}_h) + b_\tau(\boldsymbol{v}_h, \boldsymbol{v}_h).$$

We have

$$a(\boldsymbol{v}_h, \boldsymbol{v}_h) = (\boldsymbol{v}_1, \mathbf{curl}\, \boldsymbol{v}_2)_{\mathcal{T}_h} - (\boldsymbol{v}_1, \mathbf{curl}\, \boldsymbol{v}_2)_{\mathcal{T}_h} = 0,$$

and

$$
\begin{aligned}
b_\tau(\boldsymbol{v}_h, \boldsymbol{v}_h) = &-\left\langle \mathbf{n} \times \boldsymbol{v}_1^+, \boldsymbol{v}_2^+ \right\rangle_{\mathcal{F}_h^I} + \left\langle \mathbf{n} \times \boldsymbol{v}_1^-, \boldsymbol{v}_2^- \right\rangle_{\mathcal{F}_h^I} - \int_{\partial \Omega} (\mathbf{n} \times \boldsymbol{v}_1) \cdot \boldsymbol{v}_2 \\
&+ \frac{1}{2} \left\langle \boldsymbol{v}_2^+, \mathbf{n} \times \boldsymbol{v}_1^+ \right\rangle_{\mathcal{F}_h^I} - \frac{1}{2} \left\langle \boldsymbol{v}_2^+, \mathbf{n} \times \boldsymbol{v}_1^- \right\rangle_{\mathcal{F}_h^I} + \frac{1}{2} \left\langle \boldsymbol{v}_2^-, \mathbf{n} \times \boldsymbol{v}_1^+ \right\rangle_{\mathcal{F}_h^I} \\
&- \frac{1}{2} \left\langle \boldsymbol{v}_2^-, \mathbf{n} \times \boldsymbol{v}_1^- \right\rangle_{\mathcal{F}_h^I} - \frac{1}{2} \left\langle \boldsymbol{v}_1^+, \mathbf{n} \times \boldsymbol{v}_2^+ \right\rangle_{\mathcal{F}_h^I} - \frac{1}{2} \left\langle \boldsymbol{v}_1^+, \mathbf{n} \times \boldsymbol{v}_2^- \right\rangle_{\mathcal{F}_h^I} \\
&- \frac{1}{2} \left\langle \boldsymbol{v}_1^-, \mathbf{n} \times \boldsymbol{v}_2^+ \right\rangle_{\mathcal{F}_h^I} + \frac{1}{2} \left\langle \boldsymbol{v}_1^-, \mathbf{n} \times \boldsymbol{v}_2^- \right\rangle_{\mathcal{F}_h^I} \\
&- \frac{\tau}{2} ||[\![\boldsymbol{v}_1]\!]||^2_{\mathcal{F}_h^I} - \frac{1}{2\tau} ||[\![\boldsymbol{v}_2]\!]||^2_{\mathcal{F}_h^I} + \frac{1}{\tau+1} \int_{\Gamma_a} (\mathbf{n} \times \boldsymbol{v}_1) \cdot \boldsymbol{v}_2 \\
&+ \int_{\Gamma_m} (\mathbf{n} \times \boldsymbol{v}_1) \cdot \boldsymbol{v}_2 + \frac{\tau}{\tau+1} \int_{\Gamma_a} (\mathbf{n} \times \boldsymbol{v}_1) \cdot \boldsymbol{v}_2 \\
&- \frac{\tau}{\tau+1} ||\mathbf{n} \times \boldsymbol{v}_1||^2_{\Gamma_a} - \frac{1}{\tau} ||\mathbf{n} \times \boldsymbol{v}_2||^2_{\Gamma_m} - \frac{1}{\tau+1} ||\mathbf{n} \times \boldsymbol{v}_2||^2_{\Gamma_a} \\
= &- \frac{\tau}{2} ||[\![\boldsymbol{v}_1]\!]||^2_{\mathcal{F}_h^I} - \frac{1}{2\tau} ||[\![\boldsymbol{v}_2]\!]||^2_{\mathcal{F}_h^I} - \frac{\tau}{\tau+1} ||\mathbf{n} \times \boldsymbol{v}_1||^2_{\Gamma_a} \\
&- \frac{1}{\tau} ||\mathbf{n} \times \boldsymbol{v}_2||^2_{\Gamma_m} - \frac{1}{\tau+1} ||\mathbf{n} \times \boldsymbol{v}_2||^2_{\Gamma_a} \\
\leq &\,0 \quad \forall \tau > 0.
\end{aligned}
$$

This result shows the L^2-stability of the semi-discrete method. In particular, this method is dissipative for the considered numerical trace for $\hat{\mathbf{E}}_h^t$ in (9).

3.3.3. Fully discrete stability
For the sake of simplicity, we will consider $\Gamma_a = \emptyset$ in this section.

14

Notations

Let $\mathbf{L}_h : \mathbb{V}_h \to \mathbb{V}_h; \quad \forall (\boldsymbol{\iota}, \boldsymbol{\nu}) \in \mathbb{V}_h \times \mathbb{V}_h$ we have

$$(\mathbf{L}_h \boldsymbol{\iota}, \boldsymbol{\nu}) = a(\boldsymbol{\iota}, \boldsymbol{\nu}) + b_\tau(\boldsymbol{\iota}, \boldsymbol{\nu}).$$

Then, from (17) we have

$$\lambda \frac{d}{dt} \upsilon_h = \mathbf{L}_h(\upsilon_h)$$

Inverse estimations [35]

$$\forall i \in \{1, \cdots, |\mathcal{T}_h|\} \quad \exists c_{1,i},\, c_{2,i} > 0; \quad ||\mathbf{curl}(\mathbf{u})||_{L^2(K_i)} \leq c_{1,i}\, h^{-1} ||\mathbf{u}||_{L^2(K_i)}$$

$$||\mathbf{u}||_{L^2(\partial K_i)} \leq c_{2,i}\, h^{-\frac{1}{2}} ||\mathbf{u}||_{L^2(K_i)} \tag{18}$$

Lemma

$$\forall \boldsymbol{\iota} \in \mathbb{V}_h,\, \exists c > 0\,,\, \text{which depends on } \tau\,; \quad \sup_{\boldsymbol{\nu} \in \mathbb{V}_h} \frac{|(\mathbf{L}_h \boldsymbol{\iota}, \boldsymbol{\nu})|}{||\boldsymbol{\nu}||_{\mathcal{T}_h}} \leq c(\tau) h^{-1} ||\boldsymbol{\iota}||_{\mathcal{T}_h} \tag{19}$$

Proof

The proof is classical. Inverse estimations are used to upper bound the operator $\mathbf{L}_h$. First an upper bound for the bilinear form a is found, and then we show how to upper bound the first term of b_τ. The other terms of b_τ can be treated in the same way.

$\forall \boldsymbol{\iota} \in \mathbb{V}_h,$

$$\sup_{\boldsymbol{\nu} \in \mathbb{V}_h} \frac{|(\mathbf{L}_h \boldsymbol{\iota}, \boldsymbol{\nu})|}{||\boldsymbol{\nu}||_{\mathcal{T}_h}} = \sup_{\boldsymbol{\nu} \in \mathbb{V}_h} \frac{|a(\boldsymbol{\iota}, \boldsymbol{\nu}) + b_\tau(\boldsymbol{\iota}, \boldsymbol{\nu})|}{||\boldsymbol{\nu}||_{\mathcal{T}_h}} \leq \sup_{\boldsymbol{\nu} \in \mathbb{V}_h} \frac{|a(\boldsymbol{\iota}, \boldsymbol{\nu})|}{||\boldsymbol{\nu}||_{\mathcal{T}_h}} + \sup_{\boldsymbol{\nu} \in \mathbb{V}_h} \frac{|b_\tau(\boldsymbol{\iota}, \boldsymbol{\nu})|}{||\boldsymbol{\nu}||_{\mathcal{T}_h}}.$$

First we have : $\forall \boldsymbol{\iota} \in \mathbb{V}_h,$

$$|a(\boldsymbol{\iota}, \boldsymbol{\nu})| = \left| \sum_{i=1}^{|\mathcal{T}_h|} (\boldsymbol{\iota}, \zeta_{K_i}(\boldsymbol{\nu}))_{K_i} \right|$$

$$\leq \sum_{i=1}^{|\mathcal{T}_h|} \left| (\boldsymbol{\iota}, \zeta_{K_i}(\boldsymbol{\nu}))_{K_i} \right|$$

$$\leq \sum_{i=1}^{|\mathcal{T}_h|} ||\boldsymbol{\iota}||_{K_i}\, ||\zeta_K(\boldsymbol{\nu})||_{K_i}$$

15

$$\leq \sum_{i=1}^{|\mathcal{T}_h|} ||\boldsymbol{\iota}||_{K_i} \left(||\mathbf{curl}(\boldsymbol{\nu}_{2/K_i})||_{K_i}^2 + ||\mathbf{curl}(\boldsymbol{\nu}_{1/K_i})||_{K_i}^2 \right)^{\frac{1}{2}}$$

$$\leq \sum_{i=1}^{|\mathcal{T}_h|} ||\boldsymbol{\iota}||_{K_i} \left(\left[c_{1,i} h^{-1} ||\boldsymbol{\nu}_{2/K_i}||_{K_i} \right]^2 + \left[c_{1,i} h^{-1} ||\boldsymbol{\nu}_{1/K_i}||_{K_i} \right]^2 \right)^{\frac{1}{2}}$$

$$\leq c_1 h^{-1} \sum_{i=1}^{|\mathcal{T}_h|} ||\boldsymbol{\iota}||_{K_i} \, ||\boldsymbol{\nu}||_{K_i} \qquad (c_1 = \max_{i \in \{1, \cdots, |\mathcal{T}_h|\}} c_{1,i})$$

$$\leq c_1 h^{-1} \left(\sum_{i=1}^{|\mathcal{T}_h|} ||\boldsymbol{\iota}||_{K_i}^2 \right)^{\frac{1}{2}} \left(\sum_{i=1}^{|\mathcal{T}_h|} ||\boldsymbol{\nu}||_{K_i}^2 \right)^{\frac{1}{2}}$$

$$\leq c_1 h^{-1} ||\boldsymbol{\iota}||_{\mathcal{T}_h} ||\boldsymbol{\nu}||_{\mathcal{T}_h}.$$

Therefore
$$\sup_{\boldsymbol{\nu} \in \mathbb{V}_h} \frac{|a(\boldsymbol{\iota}, \boldsymbol{\nu})|}{||\boldsymbol{\nu}||_{\mathcal{T}_h}} \leq c_1 h^{-1} ||\boldsymbol{\iota}||_{\mathcal{T}_h}.$$

Second we have $\forall \boldsymbol{\iota} \in \mathbb{V}_h$,

$$\begin{aligned}
|b_\tau(\boldsymbol{\iota}, \boldsymbol{\nu})| =& | \langle \{\boldsymbol{\iota}_2\}, [\![\boldsymbol{\nu}_1]\!] \rangle_{\mathcal{F}_h^I} - \frac{\tau}{2} \langle [\![\boldsymbol{\iota}_1]\!], [\![\boldsymbol{\nu}_1]\!] \rangle_{\mathcal{F}_h^I} - \langle \{\boldsymbol{\iota}_1\}, [\![\boldsymbol{\nu}_2]\!] \rangle_{\mathcal{F}_h^I} \\
& - \frac{1}{2\tau} \langle [\![\boldsymbol{\iota}_2]\!], [\![\boldsymbol{\nu}_2]\!] \rangle_{\mathcal{F}_h^I} - \frac{1}{\tau} \int_{\Gamma_m} (\mathbf{n} \times \boldsymbol{\iota}_2) \cdot (\mathbf{n} \times \boldsymbol{\nu}_2) \\
& + \int_{\Gamma_m} (\mathbf{n} \times \boldsymbol{\iota}_1) \cdot \boldsymbol{\nu}_2 | \\
\leq& \left| \langle \{\boldsymbol{\iota}_2\}, [\![\boldsymbol{\nu}_1]\!] \rangle_{\mathcal{F}_h^I} \right| + \frac{\tau}{2} \left| \langle [\![\boldsymbol{\iota}_1]\!], [\![\boldsymbol{\nu}_1]\!] \rangle_{\mathcal{F}_h^I} \right| + \left| \langle \{\boldsymbol{\iota}_1\}, [\![\boldsymbol{\nu}_2]\!] \rangle_{\mathcal{F}_h^I} \right| \\
& + \frac{1}{2\tau} \left| \langle [\![\boldsymbol{\iota}_2]\!], [\![\boldsymbol{\nu}_2]\!] \rangle_{\mathcal{F}_h^I} \right| + \frac{1}{\tau} \int_{\Gamma_m} |(\mathbf{n} \times \boldsymbol{\iota}_2) \cdot (\mathbf{n} \times \boldsymbol{\nu}_2)| \\
& + \int_{\Gamma_m} |(\mathbf{n} \times \boldsymbol{\iota}_1) \cdot \boldsymbol{\nu}_2|.
\end{aligned}$$

We want to expand the first term and all others terms are treated similarly:

$$\left| \langle \{ \boldsymbol{\iota}_2 \}, [\![\boldsymbol{\nu}_1]\!] \rangle_{\mathcal{F}_h^I} \right| = \left| \sum_{F \in \mathcal{F}_h^I} \frac{1}{2} \left\langle \boldsymbol{\iota}_2^+ + \boldsymbol{\iota}_2^-, \mathbf{n} \times (\boldsymbol{\nu}_1^+ - \boldsymbol{\nu}_1^-) \right\rangle_F \right|$$

$$\leq \sum_{F \in \mathcal{F}_h^I} \frac{1}{2} (||\boldsymbol{\iota}_2^+||_F + ||\boldsymbol{\iota}_2^-||_F)(||\boldsymbol{\nu}_1^+||_F + ||\boldsymbol{\nu}_1^-||_F)$$

$$\leq \sum_{i=1}^{|\mathcal{T}_h|} \sum_{F \in \partial K_i} \frac{1}{2} (||\boldsymbol{\iota}_2^+||_F + ||\boldsymbol{\iota}_2^-||_F)(||\boldsymbol{\nu}_1^+||_F + ||\boldsymbol{\nu}_1^-||_F)$$

$$\leq \frac{1}{2} \sum_{i=1}^{|\mathcal{T}_h|} \sum_{F \in \partial K_i} \left[||\boldsymbol{\iota}_2^+||_F \, ||\boldsymbol{\nu}_1^+||_F + ||\boldsymbol{\iota}_2^+||_F \, ||\boldsymbol{\nu}_1^-||_F + \right.$$

$$\left. ||\boldsymbol{\iota}_2^-||_F ||\boldsymbol{\nu}_1^+||_F + ||\boldsymbol{\iota}_2^-||_F ||\boldsymbol{\nu}_1^-||_F \right]$$

$$\leq \frac{1}{2} \sum_{i=1}^{|\mathcal{T}_h|} \left[4 ||\boldsymbol{\iota}_2||_{\partial K_i} \, ||\boldsymbol{\nu}_1||_{\partial K_i} + \sum_{j \in \nu_i} \left(||\boldsymbol{\iota}_2||_{\partial K_j} \, ||\boldsymbol{\nu}_1||_{\partial K_j} + \right. \right.$$

$$\left. \left. ||\boldsymbol{\iota}_2||_{\partial K_j} \, ||\boldsymbol{\nu}_1||_{\partial K_i} + ||\boldsymbol{\iota}_2||_{\partial K_i} ||\boldsymbol{\nu}_1||_{\partial K_j} \right) \right]$$

$$\leq \frac{1}{2} \sum_{i=1}^{|\mathcal{T}_h|} \left[4 ||\boldsymbol{\iota}_2||_{\partial K_i} \, ||\boldsymbol{\nu}_1||_{\partial K_i} + \sum_{j \in \nu_i} ||\boldsymbol{\iota}_2||_{\partial K_j} \, ||\boldsymbol{\nu}_1||_{\partial K_j} + \right.$$

$$\left. ||\boldsymbol{\nu}_1||_{\partial K_i} \sum_{j \in \nu_i} ||\boldsymbol{\iota}_2||_{\partial K_j} + ||\boldsymbol{\iota}_2||_{\partial K_i} \sum_{j \in \nu_i} ||\boldsymbol{\nu}_1||_{\partial K_j} \right]$$

$$\leq 2 \sum_{i=1}^{|\mathcal{T}_h|} ||\boldsymbol{\iota}_2||_{\partial K_i} \, ||\boldsymbol{\nu}_1||_{\partial K_i} + \frac{1}{2} \sum_{i=1}^{|\mathcal{T}_h|} \sum_{j \in \nu_i} ||\boldsymbol{\iota}_2||_{\partial K_j} \, ||\boldsymbol{\nu}_1||_{\partial K_j}$$

$$+ \frac{1}{2} \sum_{i=1}^{|\mathcal{T}_h|} \left(||\boldsymbol{\nu}_1||_{\partial K_i} \sum_{j \in \nu_i} ||\boldsymbol{\iota}_2||_{\partial K_j} \right) + \frac{1}{2} \sum_{i=1}^{|\mathcal{T}_h|} \left(||\boldsymbol{\iota}_2||_{\partial K_i} \sum_{j \in \nu_i} ||\boldsymbol{\nu}_1||_{\partial K_j} \right).$$

Since we are in $\mathbb{R}^3$ every K_i has 4 neighbours except the cells on the boundary ($i.e$ $|\nu_i| \leq 4$)

$$\frac{1}{2} \sum_{i=1}^{|\mathcal{T}_h|} \sum_{j \in \nu_i} ||\boldsymbol{\iota}_2||_{\partial K_j} \, ||\boldsymbol{\nu}_1||_{\partial K_j} \leq 2 \sum_{i=1}^{|\mathcal{T}_h|} ||\boldsymbol{\iota}_2||_{\partial K_i} \, ||\boldsymbol{\nu}_1||_{\partial K_i},$$

17

and we also have that

$$\frac{1}{2} \sum_{i=1}^{|\mathcal{T}_h|} \left(||\boldsymbol{\nu}_1||_{\partial K_i} \sum_{j \in \nu_i} ||\boldsymbol{\iota}_2||_{\partial K_j} \right) \leq \frac{1}{2} \left(\sum_{i=1}^{|\mathcal{T}_h|} ||\boldsymbol{\nu}_1||_{\partial K_i}^2 \right)^{\frac{1}{2}} \left(\sum_{i=1}^{|\mathcal{T}_h|} \left(\sum_{j \in \nu_i} ||\boldsymbol{\iota}_2||_{\partial K_j} \right)^2 \right)^{\frac{1}{2}}.$$

By using the well known formula $(a_1 + a_2)^2 \leq 2(a_1^2 + a_2^2)$ so by induction we have

$$\left(\sum_{i=1}^{4} a_i \right)^2 \leq 8a_1^2 + 8a_2^2 + 4a_3^2 + 2a_4^2 \leq 8 \sum_{i=1}^{4} a_i^2$$

$$\Rightarrow \left(\sum_{i=1}^{|\mathcal{T}_h|} \left(\sum_{j \in \nu_i} ||\boldsymbol{\iota}_2||_{\partial K_j} \right)^2 \right)^{\frac{1}{2}} \leq \left(\sum_{i=1}^{|\mathcal{T}_h|} 8 \sum_{j \in \nu_i} ||\boldsymbol{\iota}_2||_{\partial K_j}^2 \right)^{\frac{1}{2}} \leq 4\sqrt{2} \left(\sum_{i=1}^{|\mathcal{T}_h|} ||\boldsymbol{\iota}_2||_{\partial K_i}^2 \right)^{\frac{1}{2}},$$

which implies

$$\frac{1}{2} \sum_{i=1}^{|\mathcal{T}_h|} \left(||\boldsymbol{\nu}_1||_{\partial K_i} \sum_{j \in \nu_i} ||\boldsymbol{\iota}_2||_{\partial K_j} \right) \leq 2\sqrt{2} \left(\sum_{i=1}^{|\mathcal{T}_h|} ||\boldsymbol{\nu}_1||_{\partial K_i}^2 \right)^{\frac{1}{2}} \left(\sum_{i=1}^{|\mathcal{T}_h|} ||\boldsymbol{\iota}_2||_{\partial K_i}^2 \right)^{\frac{1}{2}}.$$

So for now we have

$$\left| \langle \{\boldsymbol{\iota}_2\}, [\![\boldsymbol{\nu}_1]\!] \rangle_{\mathcal{F}_h^I} \right| \leq 4 \sum_{i=1}^{|\mathcal{T}_h|} ||\boldsymbol{\iota}_2||_{\partial K_i} ||\boldsymbol{\nu}_1||_{\partial K_i}$$

$$+ 4\sqrt{2} \left(\sum_{i=1}^{|\mathcal{T}_h|} ||\boldsymbol{\nu}_1||_{\partial K_i}^2 \right)^{\frac{1}{2}} \left(\sum_{i=1}^{|\mathcal{T}_h|} ||\boldsymbol{\iota}_2||_{\partial K_i}^2 \right)^{\frac{1}{2}}$$

$$\leq 4(1 + \sqrt{2}) \left(\sum_{i=1}^{|\mathcal{T}_h|} ||\boldsymbol{\nu}_1||_{\partial K_i}^2 \right)^{\frac{1}{2}} \left(\sum_{i=1}^{|\mathcal{T}_h|} ||\boldsymbol{\iota}_2||_{\partial K_i}^2 \right)^{\frac{1}{2}}.$$

From the inverse estimations (18) we deduce

$$\leq 4c_2^2(1 + \sqrt{2})h^{-1} \left(\sum_{i=1}^{|\mathcal{T}_h|} ||\boldsymbol{\nu}_1||_{K_i}^2 \right)^{\frac{1}{2}} \left(\sum_{i=1}^{|\mathcal{T}_h|} ||\boldsymbol{\iota}_2||_{K_i}^2 \right)^{\frac{1}{2}}$$

$$\leq c_3 h^{-1} ||\boldsymbol{\iota}_2||_{\mathcal{T}_h} ||\boldsymbol{\nu}_1||_{\mathcal{T}_h}.$$

Since $||\boldsymbol{\iota}||_{\mathcal{T}_h} = \left(||\boldsymbol{\iota_1}||_{\mathcal{T}_h}^2 + ||\boldsymbol{\iota_2}||_{\mathcal{T}_h}^2 \right)^{\frac{1}{2}}$ and the same for $||\nu||_{\mathcal{T}_h}$ finally we have

$$\left| \langle \{\boldsymbol{\iota_2}\}, [\![\boldsymbol{\nu_1}]\!] \rangle_{\mathcal{F}_h^I} \right| \leq c_3 h^{-1} ||\boldsymbol{\iota}||_{\mathcal{T}_h} ||\boldsymbol{\nu}||_{\mathcal{T}_h}.$$

Back to b_τ we deduce that

$$|b_\tau(\boldsymbol{\iota}, \boldsymbol{\nu})| \leq c_3 \max \left(1, \frac{1}{\tau}, \frac{\tau}{2} \right) h^{-1} ||\boldsymbol{\iota}||_{\mathcal{T}_h} ||\boldsymbol{\nu}||_{\mathcal{T}_h}$$

$$\Rightarrow \sup_{\boldsymbol{\nu} \in \mathbb{V}_h} \frac{|b_\tau(\boldsymbol{\iota}, \boldsymbol{\nu})|}{||\boldsymbol{\nu}||_{\mathcal{T}_h}} \leq c_3 \max \left(1, \frac{1}{\tau}, \frac{\tau}{2} \right) h^{-1} ||\boldsymbol{\iota}||_{\mathcal{T}_h}.$$

Finally

$$\sup_{\boldsymbol{\nu} \in \mathbb{V}_h} \frac{|(\mathbf{L}_h \boldsymbol{\iota}, \boldsymbol{\nu})|}{||\boldsymbol{\nu}||_{\mathcal{T}_h}} \leq \left[c_1 + c_3 \max \left(1, \frac{\tau}{2}, \frac{1}{\tau} \right) \right] h^{-1} ||\boldsymbol{\iota}||_{\mathcal{T}_h}.$$

Remark: this proof is valid in the case of a uniform mesh. For the case of a quasi uniform mesh, i.e. $\exists \eta > 0$ (independent of h); $\forall K_i \in \mathcal{T}_h, \forall j \in \nu_i, \dfrac{h_i}{h_j} \leq \eta$, the constant $c(\tau)$ of the lemma (19) will be replaced by $c(\tau)\eta$.

Proposition
Let $\tau \geq 0$. Under a $\frac{4}{3} - CFL$ condition, i.e $\Delta t \leq c(\tau) h^{\frac{4}{3}}$, the explicit HDGTD scheme is stable in finite time for a Runge-Kutta discretisation.

Proof
Let us study the variation of the energy defined by $\mathcal{E}_h^n = \frac{1}{2} ||\boldsymbol{v}_h^n||_\lambda^2$.
We have
$$\lambda \frac{d}{dt} v_h = \mathbf{L}_h(\boldsymbol{v}_h).$$
We propose to study a Runge-Kutta discretization, namely RK2. It can be expressed in its two steps version as follows

$$\boldsymbol{\omega}^n = \boldsymbol{v}_h^n + \Delta t \lambda^{-1} \mathbf{L}_h(\boldsymbol{v}_h^n), \quad \forall n \in \mathbb{N} \tag{20}$$

$$\boldsymbol{v}_h^{n+1} = \frac{1}{2}(\boldsymbol{v}_h^n + \boldsymbol{\omega}^n) + \frac{1}{2} \Delta t \lambda^{-1} \mathbf{L}_h(\boldsymbol{\omega}^n), \quad \forall n \in \mathbb{N} \tag{21}$$

After some manipulations we can deduce that

$$||\boldsymbol{v}_h^{n+1}||_\lambda^2 - ||\boldsymbol{v}_h^n||_\lambda^2 = ||\boldsymbol{v}_h^{n+1} - \boldsymbol{\omega}^n||_\lambda^2 + \Delta t (\mathbf{L}_h(\boldsymbol{v}_h^n), \boldsymbol{v}_h^n)_{\mathcal{T}_h} + \Delta t (\mathbf{L}_h(\boldsymbol{\omega}^n), \boldsymbol{\omega}^n)_{\mathcal{T}_h} \tag{22}$$

19

Proof

We have

$$
\begin{aligned}
||\boldsymbol{v}_h^{n+1} - \boldsymbol{\omega}^n||_\lambda^2 &= (\boldsymbol{v}_h^{n+1} - \boldsymbol{\omega}^n, \boldsymbol{v}_h^{n+1} - \boldsymbol{\omega}^n)_\lambda \\
&= ||\boldsymbol{v}_h^{n+1}||_\lambda^2 - 2(\boldsymbol{v}_h^{n+1}, \boldsymbol{\omega}^n)_\lambda + (\boldsymbol{\omega}^n, \boldsymbol{\omega}^n)_\lambda \\
&= ||\boldsymbol{v}_h^{n+1}||_\lambda^2 - (\boldsymbol{v}_h^n + \boldsymbol{\omega}^n + \Delta t \lambda^{-1} \mathbf{L}_h(\boldsymbol{\omega}^n), \boldsymbol{v}_h^n + \Delta t \lambda^{-1} \mathbf{L}_h(\boldsymbol{v}_h^n))_\lambda \\
&\quad + (\boldsymbol{\omega}^n, \boldsymbol{\omega}^n)_\lambda \\
&= ||\boldsymbol{v}_h^{n+1}||_\lambda^2 - ||\boldsymbol{v}_h^n||_\lambda^2 - \underbrace{(\boldsymbol{v}_h^n, \Delta t \lambda^{-1} \mathbf{L}_h(\boldsymbol{v}_h^n))_\lambda}_{a} - \underbrace{(\boldsymbol{\omega}^n, \boldsymbol{v}_h^n)_\lambda}_{b} \\
&\quad - \underbrace{(\boldsymbol{\omega}^n, \Delta t \lambda^{-1} \mathbf{L}_h(\boldsymbol{v}_h^n))_\lambda}_{c} - \underbrace{(\boldsymbol{v}_h^n, \Delta t \lambda^{-1} \mathbf{L}_h(\boldsymbol{\omega}^n))_\lambda}_{d} \\
&\quad - \underbrace{(\Delta t \lambda^{-1} \mathbf{L}_h(\boldsymbol{\omega}^n), \Delta t \lambda^{-1} \mathbf{L}_h(\boldsymbol{v}_h^n))_\lambda}_{e} + \underbrace{(\boldsymbol{\omega}^n, \boldsymbol{\omega}^n)_\lambda}_{f} .
\end{aligned}
$$

Recall that

- $a = \Delta t (\mathbf{L}_h(\boldsymbol{v}_h^n), \boldsymbol{v}_h^n)_{\mathcal{T}_h}$

- $d + e = (\Delta t \lambda^{-1} \mathbf{L}_h(\boldsymbol{\omega}^n), \underbrace{\boldsymbol{v}_h^n + \Delta t \lambda^{-1} \mathbf{L}_h(\boldsymbol{v}_h^n)}_{\boldsymbol{\omega}^n})_\lambda$

  $\quad = \Delta t (\mathbf{L}_h(\boldsymbol{\omega}^n), \boldsymbol{\omega}^n)_{\mathcal{T}_h}$

- $-b - c + f = (\boldsymbol{\omega}^n, \underbrace{-\boldsymbol{v}_h^n - \Delta t \lambda^{-1} \mathbf{L}_h(\boldsymbol{v}_h^n)}_{-\boldsymbol{\omega}^n} + \boldsymbol{\omega}^n)_\lambda = 0$

So finally we have

$$
||\boldsymbol{v}_h^{n+1}||_\lambda^2 - ||\boldsymbol{v}_h^n||_\lambda^2 = ||\boldsymbol{v}_h^{n+1} - \boldsymbol{\omega}^n||_\lambda^2 + \underbrace{\Delta t (\mathbf{L}_h(\boldsymbol{v}_h^n), \boldsymbol{v}_h^n)_{\mathcal{T}_h} + \Delta t (\mathbf{L}_h(\boldsymbol{\omega}^n), \boldsymbol{\omega}^n)_{\mathcal{T}_h}}_{\leq 0 \,(semi-discrete)} .
$$

Furthermore from (21)

$$
\begin{aligned}
\boldsymbol{v}_h^{n+1} - \boldsymbol{\omega}^n &= \frac{1}{2} \boldsymbol{v}_h^n - \frac{1}{2} \boldsymbol{\omega}^n + \frac{1}{2} \Delta t \lambda^{-1} \mathbf{L}_h(\boldsymbol{\omega}^n) \\
&= -\frac{1}{2} \Delta t \lambda^{-1} \mathbf{L}_h(\boldsymbol{v}_h^n) + \frac{1}{2} \Delta t \lambda^{-1} \mathbf{L}_h(\boldsymbol{\omega}^n) \\
&= -\frac{1}{2} \Delta t \lambda^{-1} \mathbf{L}_h(\boldsymbol{v}_h^n - \boldsymbol{\omega}^n).
\end{aligned}
$$

So we can deduce that

$$\|\boldsymbol{v}_h^{n+1} - \boldsymbol{\omega}^n\|_\lambda^2 = \|\frac{1}{2}\Delta t \lambda^{-1} \mathbf{L}_h(\boldsymbol{v}_h^n - \boldsymbol{\omega}^n)\|_\lambda^2$$

$$= \frac{1}{4}\Delta t^2 (\lambda^{-1}\mathbf{L}_h(\boldsymbol{v}_h^n - \boldsymbol{\omega}^n), \lambda^{-1}\mathbf{L}_h(\boldsymbol{v}_h^n - \boldsymbol{\omega}^n))_\lambda$$

$$= \frac{1}{4}\Delta t^2 \|\mathbf{L}_h(\boldsymbol{v}_h^n - \boldsymbol{\omega}^n)\|_{\lambda^{-1}}^2$$

$$\leq \frac{1}{4}\Delta t^2 \|\mathbf{L}_h(\boldsymbol{v}_h^n - \boldsymbol{\omega}^n)\|_\lambda^2.$$

From the lemma (19)

$$\leq \frac{1}{4}(\Delta t c_1 h^{-1}\eta)^2 \|\boldsymbol{v}_h^n - \boldsymbol{\omega}^n\|_\lambda^2,$$

(20) yields

$$\leq \frac{1}{4}(\Delta t^2 c_1 h^{-1}\eta)^2 (\lambda^{-1}\mathbf{L}_h(\boldsymbol{v}_h^n), \lambda^{-1}\mathbf{L}_h(\boldsymbol{v}_h^n))_\lambda$$

$$\leq \frac{1}{4}(\Delta t^2 c_1 h^{-1}\eta)^2 \|\mathbf{L}_h(\boldsymbol{v}_h^n)\|_{\lambda^{-1}}^2$$

$$\leq \frac{1}{4}(\Delta t^2 c_1 h^{-1}\eta)^2 \|\mathbf{L}_h(\boldsymbol{v}_h^n)\|_\lambda^2$$

$$\leq \frac{1}{4}(\Delta t^2 c_1 h^{-1}\eta)^2 (c_2 h^{-1}\eta)^2 \|\boldsymbol{v}_h^n\|_\lambda^2$$

$$\leq \frac{1}{4}\Delta t^4 c_3 h^{-4} \|\boldsymbol{v}_h^n\|_\lambda^2.$$

We can deduce from (22) that

$$\frac{1}{2}\|\boldsymbol{v}_h^{n+1}\|_\lambda^2 - \frac{1}{2}\|\boldsymbol{v}_h^n\|_\lambda^2 \leq \frac{1}{8}\Delta t^4 c_3 h^{-4} \|\boldsymbol{v}_h^n\|_\lambda^2$$

$$\Rightarrow \mathcal{E}_h^{n+1} - \mathcal{E}_h^n \leq \frac{1}{4}\Delta t^4 c_3 h^{-4} \mathcal{E}_h^n.$$

so for $\Delta t \leq c_4 h^{\frac{4}{3}}$ we obtain by Gronwall's lemma

$$\forall n, \quad \mathcal{E}_h^{n+1} - \mathcal{E}_h^n \leq c_5 \Delta t \mathcal{E}_h^n \Rightarrow \mathcal{E}_h^n \leq e^{c_5 T}\mathcal{E}_h^0.$$

From now on, we assume that the underlying mesh is conforming (i.e. without hanging nodes) and that the interpolation degree is the same for each element K_i, i.e. $d_i = d_j = d$. In Annex , we show that for every $K_i \in \mathcal{T}_h$ the local system of semi-discrete equations can be written as

$$
\begin{cases}
\varepsilon_i \left(\mathbb{M}_i \partial_t \overline{\mathbf{E}}_i\right) + \left(\overline{\mathbb{K}}_i \times \overline{\mathbf{H}}_i\right) + \sum_{F \in \partial K_i \cap \mathcal{F}_h^I} \frac{1}{\tau_{K_i} + \tau_{K_j}} \overline{\mathbb{S}}_{F,i} \mathbf{V}^{1,i} + \\[2ex]
\sum_{F \in \partial K_i \cap \Gamma_m} \frac{1}{\tau_{K_i}} \left(\overline{\mathbb{S}}_{F,i} \mathbf{V}^{2,i}\right) + \\[2ex]
\sum_{F \in \partial K_i \cap \Gamma_a} \frac{1}{\tau_{K_i} + 1} \overline{\mathbb{S}}_{F,i} \left(\mathbf{V}^{2,i} + \mathbf{n} \times \mathbf{g^{inc}}\right) = 0, \\[2ex]
\mu_i \left(\mathbb{M}_i \partial_t \overline{\mathbf{H}}_i\right) - \left(\overline{\mathbb{K}}_i \times \overline{\mathbf{E}}_i\right) - \sum_{F \in \partial K_i \cap \mathcal{F}_h^I} \frac{\tau_{K_i} \tau_{K_j}}{\tau_{K_i} + \tau_{K_j}} \overline{\mathbb{S}}_{F,i} \mathbf{V}^{3,i} - \\[2ex]
\sum_{F \in \partial K_i \cap \Gamma_a} \frac{1}{\tau_{K_i} + 1} \overline{\mathbb{S}}_{F,i} \left(\mathbf{V}^{4,i} + \tau_{K_i} \mathbf{V}_F^{inc}\right) = 0.
\end{cases}
\tag{23}
$$

3.4. Time integration: Low-Storage Runge-Kutta (LSRK) method
For an equation of the form

$$
\partial_t u = f(t, u),
$$

the standard s-stage Runge-Kutta scheme writes

$$
\begin{cases}
K_1 = f(t_n, u^n), \\[1ex]
K_i = f\left(t_n + c_i \Delta t, u^n + \Delta t \sum_{j=1}^{i-1} a_{i,j} K_j\right) \quad \text{for } i = 2, \cdots, s, \\[1ex]
u^{n+1} = u^n + \Delta t \sum_{j=1}^{s} b_j K_j.
\end{cases}
$$

We can easily see that this scheme is a sN-storage scheme where N is the number of equations. In this situation the memory consumption can quickly become a constraining factor for large problems. A possible solution is given by Williamson [36], who shows that the RK scheme can be cast in $2N$-storage format that we will refer to a LSRK scheme

$$
\begin{cases}
u_1 = u^n \\[2ex]
\left.\begin{array}{rcl}
u_2 & = & A_k u_2 + \Delta t f(t_n + c_k \Delta t, u_1) \\
u_1 & = & u_1 + B_k u_2
\end{array}\right\} \quad \text{for } k = 1, \cdots, s \\[2ex]
u^{n+1} = u_1
\end{cases}
$$

Since Williamson [36] has demonstrated that the four-stage fourth-order (4,4) RK scheme could not, in general, be implemented in the $2N$-storage format, we will use in this paper the $\text{LSRK}(s = 5 , p = 4)$ proposed by Carpenter and Kennedy [34] . Table 1 shows the coefficients of the method.
In our case

$$u = \begin{pmatrix} \overline{\mathbf{E}} \\ \overline{\mathbf{H}} \end{pmatrix} \text{ and } f(t, u) = \begin{pmatrix} \left(\overline{\mathbb{M}}\,\overline{\varepsilon}\right)^{-1} \left[-\overline{\mathbb{K}} \times \overline{\mathbf{H}} - \overline{\mathbf{V}^1} - \overline{\mathbf{V}_1^2} - \overline{\mathbf{V}_2^2} \right] \\ \left(\overline{\mathbb{M}}\,\overline{\mu}\right)^{-1} \left[\overline{\mathbb{K}} \times \overline{\mathbf{E}} + \overline{\mathbf{V}^3} + \overline{\mathbf{V}^4} \right] \end{pmatrix}.$$

Since we work with an explicit time discretization we choose the time step as

$$\Delta t = c_p \min_{K_i \in \tau_h} \frac{V_{K_i}}{A_{K_i}},$$

where V_{K_i} and A_{K_i} are respectively the volume and the area of cell K_i and c_p is an interpolation order-dependent constant.

4. Numerical results

The time explicit HDG method presented in the previous section has been implemented in the 3D case considering conforming tetrahedral meshes.

4.1. Propagation of a standing wave in a cubic PEC cavity

In order to validate and study the numerical convergence of the proposed HDG method, we consider the propagation of an eigenmode in a source-free *i.e* $\mathbf{J} = 0$ closed cavity (Ω is the unit square) with perfectly metallic walls.

Table 1: The values of the coefficients of the LSRK(5,4) scheme.

Coeff	Value	Coeff	Value	Coeff	Value
A_1	0	B_1	$\dfrac{1432997174477}{9575080441755}$	c_1	0
A_2	$-\dfrac{567301805773}{1357537059087}$	B_2	$\dfrac{5161836677717}{1361206829357}$	c_2	$\dfrac{1432997174477}{9575080441755}$
A_3	$-\dfrac{2404267990393}{2016746695238}$	B_3	$\dfrac{1720146321549}{2090206949498}$	c_3	$\dfrac{2526269341429}{6820363962896}$
A_4	$-\dfrac{3550918686646}{2091501179385}$	B_4	$\dfrac{3134564353537}{4481467310338}$	c_4	$\dfrac{2006345519317}{3224310063776}$
A_5	$-\dfrac{1275806237668}{842570457699}$	B_5	$\dfrac{2277821191437}{14882151754819}$	c_5	$\dfrac{2802321613138}{2924317926251}$

The frequency of the wave is $f = \frac{\sqrt{3}}{2}c_0$ where c_0 is the speed of light in vacuum. The electric permittivity and the magnetic permeability are set to the constant vacuum values. The exact time-domain solution is given by

$$
\begin{cases}
E_x(x,y,z,t) & = & -\cos(\pi x)\sin(\pi y)\sin(\pi z)\cos(\omega t), \\
E_y(x,y,z,t) & = & 0, \\
E_z(x,y,z,t) & = & \sin(\pi x)\sin(\pi y)\cos(\pi z)\cos(\omega t), \\
H_x(x,y,z,t) & = & -\dfrac{\pi}{\omega}\sin(\pi x)\cos(\pi y)\cos(\pi z)\sin(\omega t), \\
H_y(x,y,z,t) & = & \dfrac{2\pi}{\omega}\cos(\pi x)\sin(\pi y)\cos(\pi z)\sin(\omega t), \\
H_z(x,y,z,t) & = & -\dfrac{\pi}{\omega}\cos(\pi x)\cos(\pi y)\sin(\pi z)\sin(\omega t),
\end{cases}
\tag{24}
$$

where the angular frequency is given by $\omega = 2\pi f$ $(\mathrm{rad \cdot s^{-1}})$. The electromagnetic field is initialized at $t = 0$ as $E_y = H_x = H_y = H_z = 0$ and

$$
\begin{cases}
E_x(x,y,z,t=0) & = & -\cos(\pi x)\sin(\pi y)\sin(\pi z), \\
E_z(x,y,z,t=0) & = & \sin(\pi x)\sin(\pi y)\cos(\pi z).
\end{cases}
\tag{25}
$$

4.1.1. Uniform $\tau = 1$

In order to insure the stability of the method, numerical CFL conditions are determined for each value of the interpolation order p_K. In our particular case the relative ε_K and μ_k are constant $= 1$ forall $K \in \mathcal{T}_h$, so we have verified that, as we said in Remark 3, for $\tau = 1$, the values of the CFL number correspond to those obained for the classical upwind flux-based DG method. In Table 2 we summarize the maximum value of Δt to insure the stability of the HDG scheme

Interpolation order	$\mathbb{P}_1$	$\mathbb{P}_2$	$\mathbb{P}_3$	$\mathbb{P}_4$
Δt max (s.)	0.32×10^{-9}	0.19×10^{-9}	0.13×10^{-9}	0.94×10^{-10}

Table 2: Numerically obtained values of Δt max.

Given these values of Δt, the L^2-norm of the error is calculated for a uniform tetrahedral mesh with 3072 elements which is constructed from a finite difference grid with $n_x = n_y = n_z = 9$ points, each cell of this grid yielding 6 tetrahedra. The wave is propagated in the cavity during a physical time $t_{\max}$ corresponding to 8 periods. Figure 1 shows the time evolution of the exact and the numerical solution of E_x at a fixed point in the mesh. Figure 2, shows $\|\mathbf{E}\|$ for 2 uniform meshes, the first is constituted by 384 elements and the second by 3072 elements, for $p_K = 4$. Figures 3 and 4 depicts a comparison of the time evolution of the L^2-norm of the error between the solution obtained

with an HDG method and a classical upwind flux-based DG method for different values of the interpolation order. An optimal convergence with order $p_K + 1$ is obtained as shown in Figure 5.
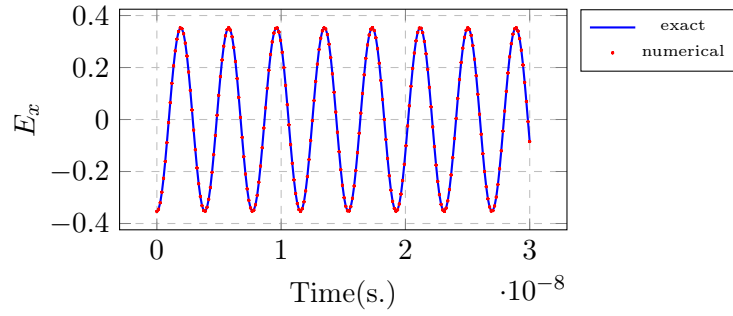

Figure 1: Time evolution of the exact and the numerical solution of E_x at point $A(0.25, 0.25, 0.25)$ with a $\mathbb{P}_3$ interpolation.
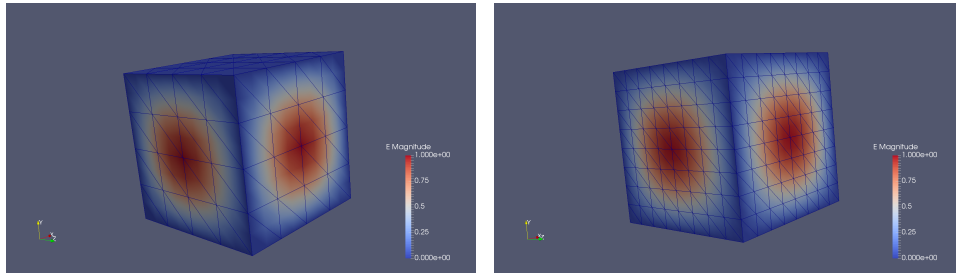

Figure 2: The magnitude of E at a fixed time for two uniform meshes constituted by 384 and 3072 elements with a $\mathbb{P}_4$ interpolation.
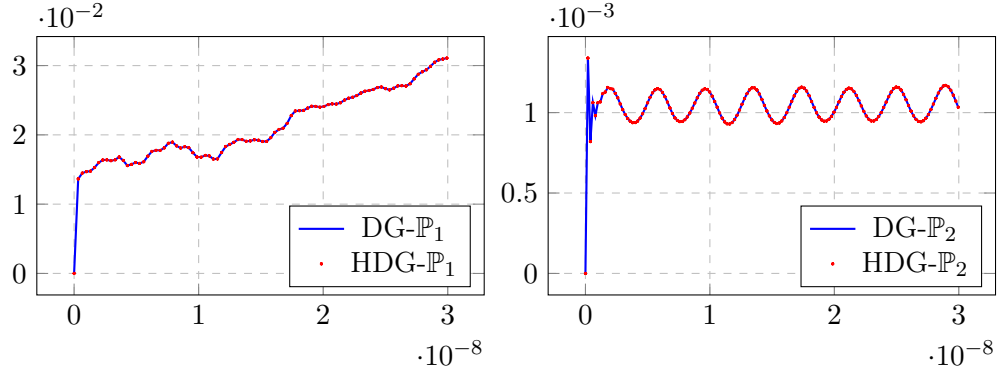
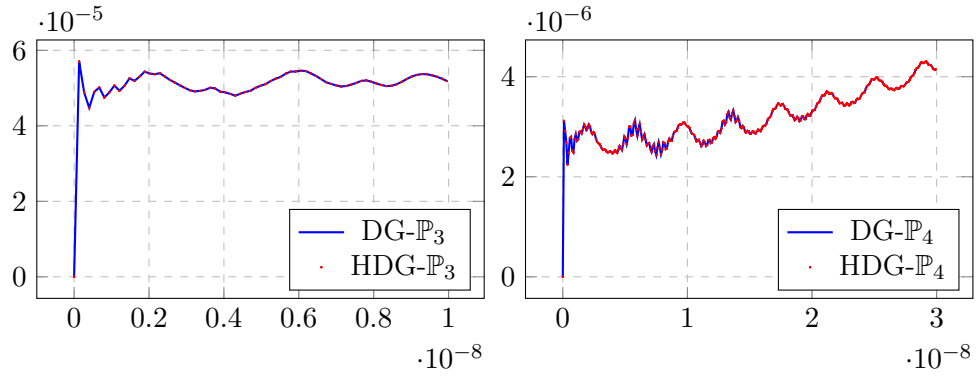Figure 3: Time evolution of the L^2-norm of the error for $\mathbb{P}_1$ and $\mathbb{P}_2$.

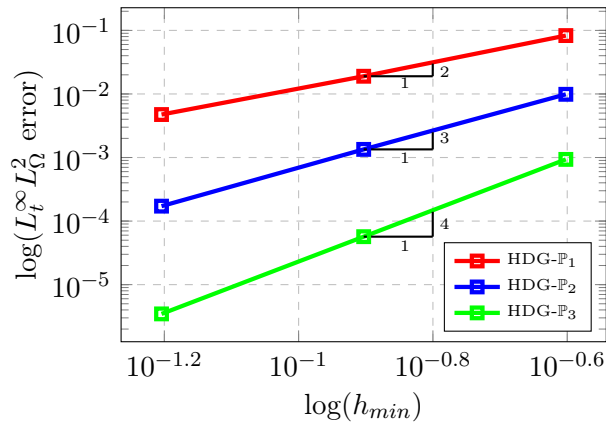Figure 4: Time evolution of the L^2-norm of the error for $\mathbb{P}_3$ and $\mathbb{P}_4$.

Figure 5: Numerical convergence order of the time explicit HDG method for $\tau = 1$.

4.1.2. Influence of τ

We keep the same case than previously and we assess the behavior of the HDG method for various values of the penalization parameter τ. We have seen in the fully discrete stability analysis that the CFL number depends on τ, and numerically when we fixed Δt to the value shown in Table 2 (corresponding to $\tau = 1$) but changed the value of τ we observed that the time evolution of the electromagnetic energy increases in time for any order of interpolation . In fact, it is necessary to reevaluate the Δt max for each value of τ (see Figure 6). On Figure 7, we show the time evolution of the L^2-error for several values of τ with respect to the maximal Δt for the considered parameters. In addition, Table 4 summarizes the numerical results in term of maximum L^2-errors and convergence rates. It appears that the order of convergence is not affected when we change the stabilization parameter (with their associated CFL conditions).

Tau	0.1	1.0	2.0	5.0	10.0
Δt max (sec)	0.31×10^{-10}	0.32×10^{-9}	0.17×10^{-9}	0.66×10^{-10}	0.32×10^{-10}

Table 3: Numerically obtained values of the CFL number as a function of the stabilization parameter τ for a $\mathbb{P}1$ interpolation.
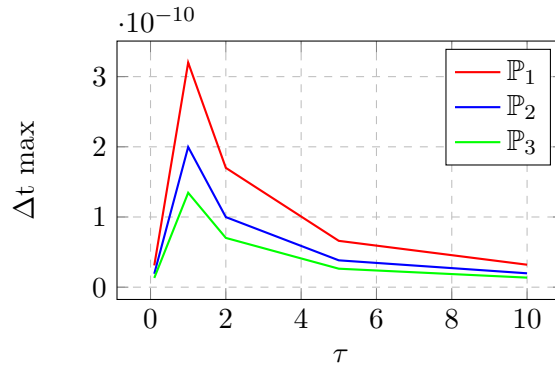

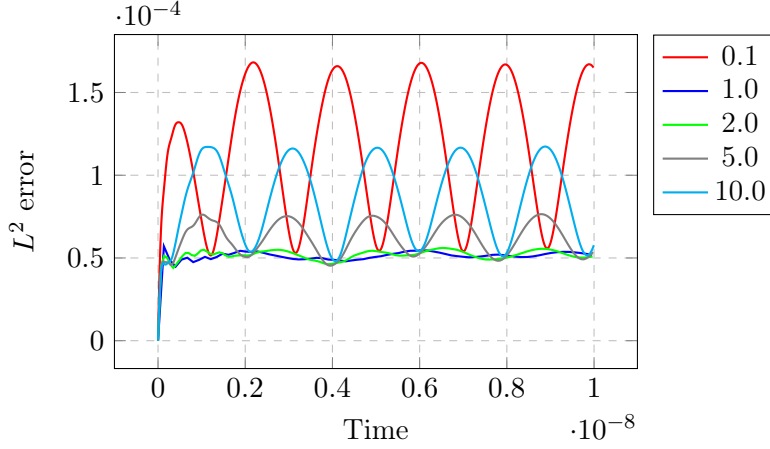Figure 6: Variation of the Δt max as a function of τ.

Figure 7: Time evolution of the L^2-error as a function of τ with a $\mathbb{P}_3$ interpolation.

| $1/h$ | $\tau = 1.0$ | | | | | |
	$\mathbb{P}_1$, $\Delta t = 0.16 \times 10^{-09}$		$\mathbb{P}_2$, $\Delta t = 0.99 \times 10^{-10}$		$\mathbb{P}_3$, $\Delta t = 0.66 \times 10^{-10}$	
1/4	8.29e-02	-	9.87e-03	-	9.34e-04	-
1/8	1.90e-02	**2.13**	1.34e-03	**2.88**	5.68e-05	**4.04**
1/16	4.74e-03	**2.00**	1.72e-04	**2.97**	3.46e-06	**4.04**

| $1/h$ | $\tau = 0.1$ | | | | | |
	$\mathbb{P}_1$, $\Delta t = 0.16 \times 10^{-10}$		$\mathbb{P}_2$, $\Delta t = 0.96 \times 10^{-11}$		$\mathbb{P}_3$, $\Delta t = 0.66 \times 10^{-11}$	
1/4	2.14e-01	-	1.78e-02	-	2.19e-03	-
1/8	5.46e-02	**1.97**	2.85e-03	**2.65**	1.68e-04	**3.70**
1/16	1.18e-02	**2.21**	4.06e-04	**2.81**	1.14e-05	**3.88**

| $1/h$ | $\tau = 10.0$ | | | | | |
	$\mathbb{P}_1$, $\Delta t = 0.16 \times 10^{-10}$		$\mathbb{P}_2$, $\Delta t = 0.96 \times 10^{-11}$		$\mathbb{P}_3$, $\Delta t = 0.68 \times 10^{-11}$	
1/6	1.74e-01	-	1.53e-02	-	1.68e-03	-
1/12	4.24e-02	**2.04**	2.23e-03	**2.76**	1.17e-04	**3.84**
1/24	9.4e-03	**2.16**	3.10e-04	**2.87**	7.81e-06	**3.91**

Table 4: Maximum L^2-errors and convergence orders.

4.2. Propagation of a plane wave in a homogeneous domain

We now consider the propagation of a plane wave in a homogeneous domain. $\mathbf{E}_0$ and $\mathbf{k}$ are the polarisation and the wave vector. The electric permittivity and the magnetic permeability are set to the constant vacuum

values. The exact time-domain solution is given by

$$
\begin{cases}
\mathbf{E}(\mathbf{x}, t) &= \mathbf{E}_0 \left(t - \sqrt{\mu_r \varepsilon_r} \dfrac{\mathbf{k} \cdot \mathbf{x}}{|\mathbf{k}|} \right), \\[2em]
\mathbf{H}(\mathbf{x}, t) &= \sqrt{\dfrac{\varepsilon_r}{\mu_r}} \dfrac{\mathbf{k}}{|\mathbf{k}|} \times \mathbf{E}(\mathbf{x}, t).
\end{cases}
$$

Figure 8 shows the time evolution of the exact and the numerical solution of E_x at a fixed point in the domain. An optimal convergence with order $p_K + 1$ is obtained as shown in Figure 9. Figure 10 shows the time evolution of the L^2-norm of the error with different polynomial orders.
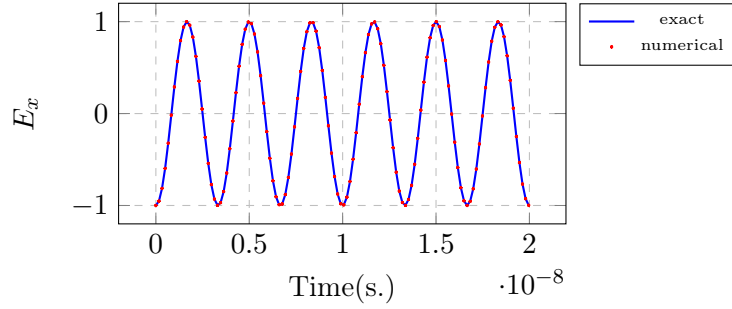

Figure 8: Time evolution of the exact and the numerical solution of E_x at point $A(0.25, 0.25, 0.25)$ with a $\mathbb{P}_3$ interpolation.
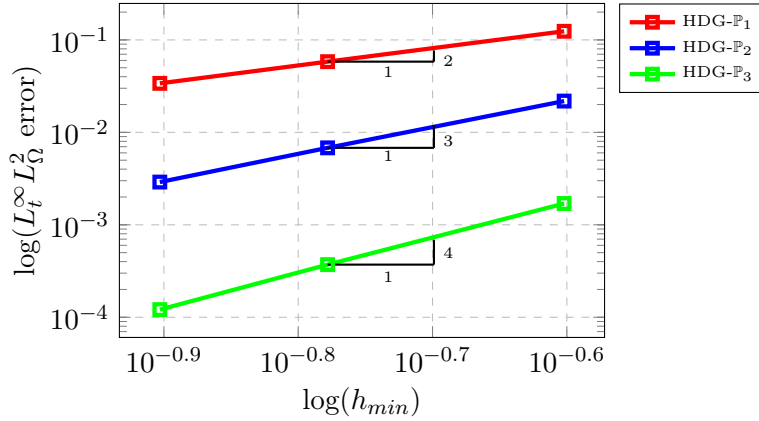

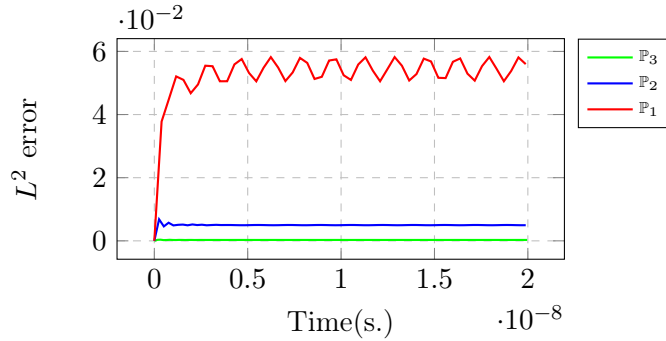Figure 9: Numerical convergence order of the time explicit HDG method for $\tau = 1$.

29

Figure 10: Time evolution of the L^2-norm of the error for $\mathbb{P}_1$, $\mathbb{P}_2$ and $\mathbb{P}_3$.

4.3. Scattering of a plane wave by a dielectric sphere

We now consider a problem involving a dielectric sphere of radius 0.15 meter, with $\varepsilon_r = 2$ and $\mu_r = 1$. The computational domain is bounded by a cube of side 1 meter on which the Silver-Muller absorbing condition is applied. A plane wave traveling in the z direction is considered, impinging in normal incidence from the bottom. The numerical simulation is computed for polynomial order $\mathbb{P}_1$ on a coarse mesh and $\mathbb{P}_4$ on a fine mesh (as seen in Figure 11) with the particular stabilization parameter $\tau_K = \sqrt{\mu_K}/\sqrt{\varepsilon_K}$. The solution obtained for $\mathbb{P}_4$ on a fine mesh will be considered as a reference solution since we do not have access to the analytical solution in this case. The first tetrahedral mesh consists of 9227 elements, 96 elements for the sphere, and the rest for the vacuum for $\mathbb{P}_1$ (Figure 11 left) and another tetrahedral mesh which consists of 32602 elements, 565 elements for the sphere, the rest for the vacuum for $\mathbb{P}_4$ (Figure 11 right). The simulation is computed on 22 cores, it takes 1 minute and 42 seconds for 136 time-steps in the case of $\mathbb{P}_1$ interpolation with the first mesh, and takes 3 hours and 23 minutes for 699 time-steps in the case of $\mathbb{P}_4$ interpolation with the second mesh.
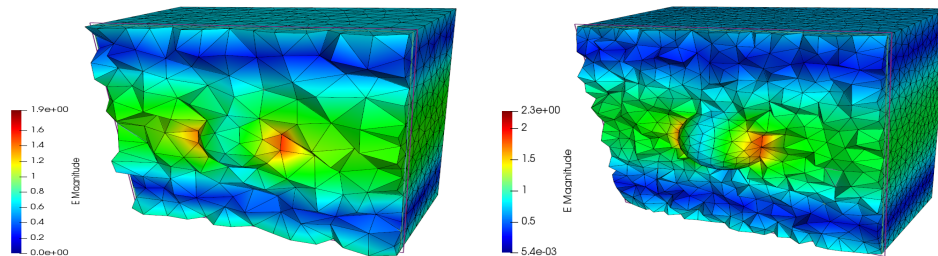

Figure 11: Snapshot of the 3D simulation of the norm of the the electric field at a fixed time for P_1 interpolation (left) and P_4 interpolation (right).

30

5. Local postprocessing

5.1. Definition

The $L^2(\mathcal{T}_h)$ and $H_{curl}(\mathcal{T}_h)$ norms of a vector field are defined by

$$||\cdot||_{L^2(\mathcal{T}_h)} = \sum_{K \in \mathcal{T}_h} ||\cdot||_{L^2(K)},$$

$$||\cdot||_{H_{curl}(\mathcal{T}_h)} = \sum_{K \in \mathcal{T}_h} ||\cdot||_{L^2(K)} + ||\nabla \times \cdot||_{L^2(K)}.$$

5.2. Motivation

The local postprocessing method consists of finding new approximations for the electric and magnetic field $\mathbf{E}_h^{n*}$ and $\mathbf{H}_h^{n*}$ that both converge with order $k+1$ in the $L^2(\mathcal{T}_h)$ norm and in the $H^{curl}(\mathcal{T}_h)$ norm, whereas $\mathbf{E}_h^n$ and $\mathbf{H}_h^n$ converge with order $k+1$ in the $L^2(\mathcal{T}_h)$ norm but with order k in the $H^{curl}(\mathcal{T}_h)$ norm. It is worth to note out that we can deduce the new approximations $\mathbf{E}_h^{n*}$ and $\mathbf{H}_h^{n*}$ directly from $\mathbf{E}_h^n$ and $\mathbf{H}_h^n$ at any time step between $[0, T]$ without knowing the value of $\mathbf{E}_h^{(n-1)*}$ and $\mathbf{H}_h^{(n-1)*}$. Hence, the local postprocessing can be performed whenever higher accuracy is needed at particular time steps. Following the ideas of the local postprocessing developped in [37] for Maxwell equations in frequency-domain and the one that has been developed in [33] for acoustic wave equation in time-domain, we end up with the formulation shown below.

5.3. Formulation

We first compute an approximation $(\mathbf{p}_{1,h}^n, \mathbf{p}_{2,h}^n) \in \mathbf{V}(K) \times \mathbf{V}(K)$ to the curl of $\mathbf{E}$, $\mathbf{p}_1(t^n) = \nabla \times \mathbf{E}(t^n)$ and the curl of $\mathbf{H}$, $\mathbf{p}_2(t^n) = \nabla \times \mathbf{H}(t^n)$ by locally solving the below system

$$(\mathbf{p}_{1,h}^n, \mathbf{v})_K = (\mathbf{E}_h^n, \nabla \times \mathbf{v})_K - \langle \hat{\mathbf{E}}_h^{t,n}, \mathbf{n} \times \mathbf{v} \rangle_{\partial K} \quad \forall \mathbf{v} \in \mathbf{V}(K),$$

and

$$(\mathbf{p}_{2,h}^n, \mathbf{v})_K = (\mathbf{H}_h^n, \nabla \times \mathbf{v})_K - \langle \hat{\mathbf{H}}_h^{t,n}, \mathbf{n} \times \mathbf{v} \rangle_{\partial K} \quad \forall \mathbf{v} \in \mathbf{V}(K).$$

We then find $(\mathbf{E}_h^{n*}, \mathbf{H}_h^{n*}) \in [\mathcal{P}_{k+1}(K)]^3 \times [\mathcal{P}_{k+1}(K)]^3$ such that

$$\begin{cases} (\nabla \times \mathbf{E}_h^{n*}, \nabla \times \mathbf{W})_K = (\mathbf{p}_{h,1}^n, \nabla \times \mathbf{W})_K, & \forall \mathbf{W} \in [\mathcal{P}_{k+1}(K)]^3, \\ (\mathbf{E}_h^{n*}, \nabla Y)_K = (\mathbf{E}_h^n, \nabla Y)_K & \forall Y \in \mathcal{P}_{k+2}(K). \end{cases}$$

and

$$\begin{cases} (\nabla \times \mathbf{H}_h^{n*}, \nabla \times \mathbf{W})_K = (\mathbf{p}_{h,2}^n, \nabla \times \mathbf{W})_K, & \forall \mathbf{W} \in [\mathcal{P}_{k+1}(K)]^3, \\ (\mathbf{H}_h^{n*}, \nabla Y)_K = (\mathbf{H}_h^n, \nabla Y)_K & \forall Y \in \mathcal{P}_{k+2}(K). \end{cases}$$
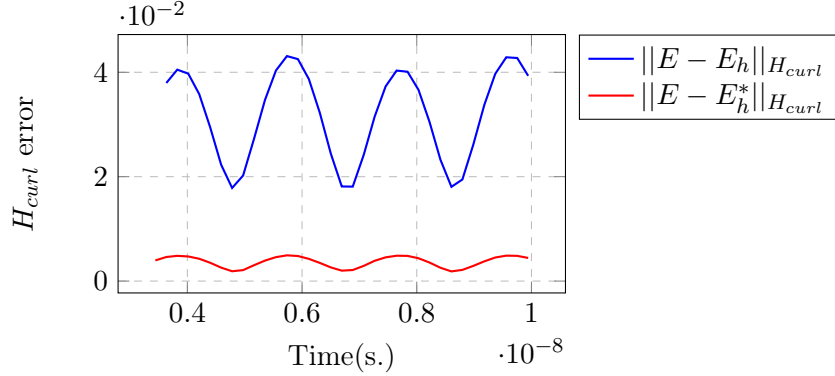
Figure 12: Time evolution of the H_{curl}-error before and after postprocessing for P_2 interpolation and a fixed mesh constituted by 3072 elements.

5.4. Numerical results

5.4.1. Propagation of a standing wave in a cubic PEC cavity

The numerical results given here are for the electric field only in the cubic cavity case. The postprocessing works for the magnetic field similarly. Figure 13 shows that the H^{curl} error for the new solution is smaller than before. Table 5 shows that a $k + 1$ order convergence rate is obtained for the post processed solution instead of k as expected.

		$\tau = 1.0$							
		$\|\|E - E_h\|\|_{L^2}$		$\|\|E - E_h^*\|\|_{L^2}$		$\|\|E - E_h\|\|_{H_{curl}}$		$\|\|E - E_h^*\|\|_{H_{curl}}$	
P_k	$1/h$	Error	order	Error	order	Error	order	Error	order
	1/4	7.50e-02	-	1.19e-01	-	9.30e-01	-	6.83e-01	-
P_1	1/6	3.20e-02	**2.10**	5.37e-02	**1.97**	5.84e-01	**1.14**	3.10e-01	**1.95**
	1/8	1.70e-02	**2.19**	2.86e-02	**2.19**	4.34e-01	**1.03**	1.67e-01	**2.15**
	1/4	8.60e-03	-	5.80e-03	-	1.67e-01	-	4.28e-02	-
P_2	1/6	2.80e-03	**2.77**	1.50e-03	**3.33**	7.46e-02	**1.98**	1.19e-02	**3.16**
	1/8	1.20e-03	**2.95**	6.06e-04	**3.18**	4.29e-02	**1.92**	4.90e-03	**3.06**
	1/4	7.98e-04	-	5.22e-04	-	2.30e-02	-	5.00e-03	-
P_3	1/6	1.57e-04	**4.00**	1.12e-04	**3.78**	7.10e-03	**2.90**	1.10e-03	**3.79**
	1/8	5.04e-05	**3.95**	3.66e-05	**3.90**	3.00e-03	**2.99**	3.58e-04	**3.84**

Table 5: Maximum L^2 & H^{curl}-errors and convergence orders.

5.4.2. Scattering of a plane wave by a dielectric sphere

To validate the superconvergence we will compute the L^2 error in time of $[\nabla \times E]_x$, $[\nabla \times E]_y$, $[\nabla \times E]_z$ between the solution calculated by the approximation P_2 before and after postprocessing and the reference solution P_4 mentioned in 4.3.

In other terms we will compute, for $\nu \in \{x, y, z\}$

$$err = \sum_{i=\Delta t}^{N\Delta t} \left| [\nabla \times E]_{\nu, P_4}(i, x_A, y_A, z_A) - [\nabla \times E]_{\nu, P_2}(i, x_A, y_A, z_A) \right|^2,$$

and

$$err_{PP} = \sum_{i=\Delta t}^{N\Delta t} \left| [\nabla \times E]_{\nu, P_4}(i, x_A, y_A, z_A) - [\nabla \times E]_{\nu, P_{2PP}}(i, x_A, y_A, z_A) \right|^2,$$

while $[\nabla \times E]_{\nu, P_2}$ and $[\nabla \times E]_{\nu, P_{2PP}}$ are the solutions with approximation P_2 before and after postprocessing respectively. A is a probe point in the domain.

We will consider 7 points in all directions, see Figure 13, to validate the postprocessing technique on the curl of the approximation. Table 6 shows that $err_{PP} \leq err$ in almost all cases. The characteristics of the mesh are the same as in figure 11 (right).
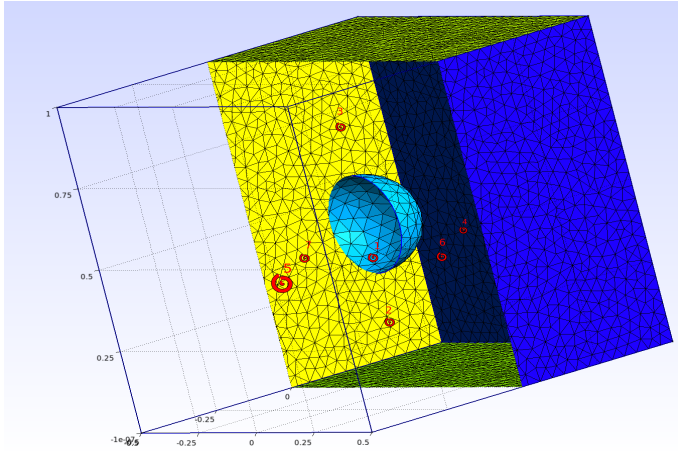

Figure 13: The positions of the probe points.

Points	components	err	err_{PP}
$A_1(0,0,0.4)$	$[\nabla \times E]_x$	**0.2124**	**0.1846**
	$[\nabla \times E]_y$	**3.2110**	**2.5513**
	$[\nabla \times E]_z$	**0.3597**	**0.3092**
$A_2(0,0,0.2)$	$[\nabla \times E]_x$	**0.0356**	**0.0356**
	$[\nabla \times E]_y$	**0.8186**	**0.6761**
	$[\nabla \times E]_z$	**0.0378**	**0.0388**
$A_3(0,0,0.8)$	$[\nabla \times E]_x$	**0.0826**	**0.0598**
	$[\nabla \times E]_y$	**0.8028**	**0.7280**
	$[\nabla \times E]_z$	**0.2153**	**0.1558**
$A_4(0.3,0,0.4)$	$[\nabla \times E]_x$	**0.1633**	**0.1195**
	$[\nabla \times E]_y$	**1.2381**	**0.4381**
	$[\nabla \times E]_z$	**0.1224**	**0.1179**
$A_5(-0.3,0,0.4)$	$[\nabla \times E]_x$	**0.0430**	**0.0396**
	$[\nabla \times E]_y$	**0.5975**	**0.3552**
	$[\nabla \times E]_z$	**0.0552**	**0.0412**
$A_6(0,0.3,0.4)$	$[\nabla \times E]_x$	**0.0579**	**0.0373**
	$[\nabla \times E]_y$	**0.5968**	**0.3581**
	$[\nabla \times E]_z$	**1.0404**	**1.0649**
$A_7(0,-0.3,0.4)$	$[\nabla \times E]_x$	**0.0412**	**0.0374**
	$[\nabla \times E]_y$	**0.5900**	**0.3513**
	$[\nabla \times E]_z$	**1.0312**	**1.1060**

Table 6: L^2 error between the reference solution and the solution P_2 before and after postprocessing of all the components

6. Conclusion

We have formulated a fully explicit HDG method for the 3D time-domain Maxwell equations and proved the semi and fully-discrete stability of the scheme. The method can be seen as a generalization of the classical DGTD scheme based on upwind fluxes. It coincides with the latter scheme for a particular choice of the stabilization parameter τ introduced in the definition of numerical traces in the HDG framework . We have assessed numerically the influence of this parameter on the scheme and we presented the numerical solution of Maxwell equations in the case of propagation of a standing wave in a cubic PEC cavity, propagation of a plane wave in a homogeneous domain and scattering of a plane wave by a dielectric sphere.
The method posseses a superconvergence property, which allows us, by means of local postprocessing, to obtain new improved approximations of the variables at any time levels. In particular, the new approximations converge with order $k + 1$ instead of k in the H^{curl}-norm for $k \geq 1$. We have shown the results of the post processing in a case which has an analytical solution (cubic cavity) and in another case which has not (dielectric sphere). The next step is to couple explicit and implicit HDG methods to treat the case of a locally refined meshes.

Annex

In this section we will present all the details to elaborate the explicit HDGTD method.

Local HDG weak form

We assume that for an internal interface $F = \overline{K}^+ \cap \overline{K}^-$, the normal vector $\mathbf{n} = \mathbf{n}^+ = -\mathbf{n}^-$ is directed from K^+ to K^-. For a boundary interface, we implicitly have that $\mathbf{n} = \mathbf{n}^+$ and we simply denote by K in place of K^+ the element attached to the interface. Replacing the numerical traces (12) and (13) in (14) we obtain

$$
\begin{cases}
(\varepsilon \partial_t \mathbf{E}_h, \mathbf{v})_K - (\mathbf{H}_h, \mathbf{curl}\, \mathbf{v})_K \\[2mm]
\quad + \sum_{F \in \partial K \cap \mathcal{F}_h^I} \left\langle \frac{1}{\tau_{K^+} + \tau_{K^-}} \left(\tau_{K^+} \mathbf{H}_h^{t,+} + \tau_{K^-} \mathbf{H}_h^{t,-} \right) \mathbf{n} \times \mathbf{v} \right\rangle_F \\[2mm]
\quad + \sum_{F \in \partial K \cap \mathcal{F}_h^I} \left\langle \frac{1}{\tau_{K^+} + \tau_{K^-}} \left(\mathbf{n}^+ \times \mathbf{E}_h^{t,+} + \mathbf{n}^- \times \mathbf{E}_h^{t,-} \right), \mathbf{n} \times \mathbf{v} \right\rangle_F \\[2mm]
\quad + \sum_{F \in \partial K \cap \Gamma_m} \left\langle \frac{1}{\tau_K} \mathbf{n} \times \mathbf{E}_h^t + \mathbf{H}_h^t, \mathbf{n} \times \mathbf{v} \right\rangle_F \\[2mm]
\quad + \sum_{F \in \partial K \cap \Gamma_a} \left\langle \frac{1}{\tau_K + 1} \left(\tau_K \mathbf{H}_h^t + \mathbf{n} \times \mathbf{E}_h^t - \mathbf{g}^{inc} \right), \mathbf{n} \times \mathbf{v} \right\rangle_F = 0, \\[4mm]
(\mu \partial_t \mathbf{H}_h, \mathbf{v})_K + (\mathbf{E}_h, \mathbf{curl}\, \mathbf{v})_K - \\[2mm]
\quad \sum_{F \in \partial K \cap \mathcal{F}_h^I} \left\langle \frac{\tau_{K^+} \tau_{K^-}}{\tau_{K^+} + \tau_{K^-}} \left(\frac{\mathbf{E}_h^{t,+}}{\tau_{K^+}} + \frac{\mathbf{E}_h^{t,-}}{\tau_{K^-}} - \mathbf{n}^+ \times \mathbf{H}_h^{t,+} - \mathbf{n}^- \times \mathbf{H}_h^{t,-} \right), \mathbf{n} \times \mathbf{v} \right\rangle_F \\[2mm]
\quad - \sum_{F \in \partial K \cap \Gamma_a} \left\langle \frac{1}{\tau_K + 1} \left(\mathbf{E}_h^t - \tau_K \mathbf{n} \times \mathbf{H}_h^t - \tau_K \mathbf{n} \times \mathbf{g}^{inc} \right), \mathbf{n} \times \mathbf{v} \right\rangle_F = 0.
\end{cases}
\tag{26}
$$

where $\mathbf{H}_h^{t,+}$ and $\mathbf{E}_h^{t,+}$ $\left(\text{respectively } \mathbf{H}_h^{t,-} \text{ and } \mathbf{E}_h^{t,-}\right)$ are the tagential traces of $\mathbf{H}_h$ and $\mathbf{E}_h$ from element K^+ (respectively K^-).

Local HDG matrices

Let $\mathcal{T}_h$ be the set of all K_i with $i \in \{1, \cdots, |\mathcal{T}_h|\}$, and let d_i be the number of degrees of freedom in element K_i. From now on, for a given element $K_i \in \mathcal{T}_h$, we consider that $K^+ \equiv K_i$ and $K^- \equiv K_j$. We define the restricted fields

$\mathbf{E}_i = \mathbf{E}_{h_{|K_i}} = \begin{pmatrix} E_i^x \\ E_i^y \\ E_i^z \end{pmatrix}$ and $\mathbf{H}_i = \mathbf{H}_{h_{|K_i}} = \begin{pmatrix} H_i^x \\ H_i^y \\ H_i^z \end{pmatrix}$. We will now develop the equation for E_i^x in (26) in order to exhibit the local matrices characterizing the semi-discrete HDG scheme. Let $(\Phi_{ik})_{1 \leq k \leq d_i}$ be the set of scalar basis functions defined in K_i. By setting $\mathbf{v} = \boldsymbol{\Phi}_{ik}^x = \begin{pmatrix} \Phi_{ik} \\ 0 \\ 0 \end{pmatrix}$ for $1 \leq k \leq d_i$ the equation for E_i^x in (26) becomes

$$
\int_{K_i} \varepsilon \partial_t E_i^x \Phi_{ik} - \int_{K_i} (H_i^y \partial_z \Phi_{ik} - H_i^z \partial_y \Phi_{ik}) \ +
$$

$$
\sum_{F \in \partial K_i \cap \mathcal{F}_h^I} \int_F \frac{1}{\tau_{K_i} + \tau_{K_j}} \left[\tau_{K_i} H_i^{t,y} + \tau_{K_j} H_j^{t,y} + \right.
$$

$$
\left. \left(\mathbf{n}^+ \times \mathbf{E}_i^t\right)^y + \left(\mathbf{n}^- \times \mathbf{E}_j^t\right)^y \right] n_z \Phi_{ik} \ -
$$

$$
\frac{1}{\tau_{K_i} + \tau_{K_j}} \left[\tau_{K_i} H_i^{t,z} + \tau_{K_j} H_j^{t,z} + \right.
$$

$$
\left. \left(\mathbf{n}^+ \times \mathbf{E}_i^t\right)^z + \left(\mathbf{n}^- \times \mathbf{E}_j^t\right)^z \right] n_y \Phi_{ik} \ + \tag{27}
$$

$$
\sum_{F \in \partial K_i \cap \Gamma_m} \int_F \left(\frac{1}{\tau} \left(\mathbf{n} \times \mathbf{E}_i^t\right)^y + H_i^{t,y} \right) n_z \Phi_{ik} -
$$

$$
\left(\frac{1}{\tau} \left(\mathbf{n} \times \mathbf{E}_i^t\right)^z + H_i^{t,z} \right) n_y \Phi_{ik} \ +
$$

$$
\sum_{F \in \partial K_i \cap \Gamma_a} \int_F \frac{1}{\tau_{K_i} + 1} \left(\tau_{K_i} H_i^{t,y} + \left(\mathbf{n} \times \mathbf{E}_i^t\right)^y - g^{inc,y} \right) n_z \Phi_{ik} -
$$

$$
\frac{1}{\tau_{K_i} + 1} \left(\tau_{K_i} H_i^{t,z} + \left(\mathbf{n} \times \mathbf{E}_i^t\right)^z - g^{inc,z} \right) n_y \Phi_{ik} = 0.
$$

Note that we obtain d_i equations of the form (27), one for each value of k. The different terms appearing in (27) can be developed as follows.

- Mass matrix. Assuming that ε is constant on every K_i, we obtain

$$
\begin{aligned}
\int_{K_i} \varepsilon_i \partial_t E_i^x \Phi_{ik} &= \varepsilon_i \int_{K_i} \sum_{l=1}^{d_i} \partial_t E_{il}^x \Phi_{il} \Phi_{ik} \\
&= \varepsilon_i \sum_{l=1}^{d_i} \partial_t E_{il}^x \int_{K_i} \Phi_{il} \Phi_{ik} \\
&= \varepsilon_i \left(\mathbb{M}_i \partial_t \overline{\mathbf{E}}_i^x \right)_k, \quad 1 \le k \le d_i,
\end{aligned}
\tag{28}
$$

where $\mathbb{M}_i$ is the mass matrix, of dimension $d_i \times d_i$

$$
\mathbb{M}_i = \left(\int_{K_i} \Phi_{il} \Phi_{ik} \right)_{1 \le l, k \le d_i},
$$

and assuming that the vector of all the degrees of freedom of $\mathbf{E}$ in K_i has been ordered as

$$
\overline{\mathbf{E}}_i = \begin{pmatrix} \overline{\mathbf{E}}_i^x \\ \overline{\mathbf{E}}_i^y \\ \overline{\mathbf{E}}_i^z \end{pmatrix} = \begin{pmatrix} (E_{il}^x)_{1 \le l \le d_i} \\ (E_{il}^y)_{1 \le l \le d_i} \\ (E_{il}^z)_{1 \le l \le d_i} \end{pmatrix}.
$$

- Stiffness matrix.

$$
\begin{aligned}
\int_{K_i} H_i^y \partial_z \Phi_{ik} - H_i^z \partial_y \Phi_{ik} &= \int_{K_i} \sum_{l=1}^{d_i} \left(H_{il}^y \Phi_{il} \, \partial_z \Phi_{ik} - H_{il}^z \Phi_{il} \, \partial_y \Phi_{ik} \right) \\
&= \sum_{l=1}^{d_i} H_{il}^y \int_{K_i} \Phi_{il} \, \partial_z \Phi_{ik} - \sum_{l=1}^{d_i} H_{il}^z \int_{K_i} \Phi_{il} \, \partial_y \Phi_{ik} \\
&= \left(\mathbb{K}_i^z \overline{\mathbf{H}}_i^y - \mathbb{K}_i^y \overline{\mathbf{H}}_i^z \right)_k \\
&= - \left(\mathbb{K}_i \times \overline{\mathbf{H}}_i \right)_k^x, \quad 1 \le k \le d_i.
\end{aligned}
\tag{29}
$$

Here, the three stiffness matrices were introduced

$$
(\mathbb{K}_i^\nu) = \left(\int_{K_i} \Phi_{il} \, \partial_\nu \, \Phi_{ik} \right)_{1 \le l, k \le d_i} \qquad \text{for } \nu \in \{x, y, z\},
$$

37

and where we have introduced the $3d_i \times d_i$ stiffness matrix that will be used in the final system

$$\overline{\mathbb{K}}_i = \left[\begin{array}{c} \mathbb{K}_i^x \\ \mathbb{K}_i^y \\ \mathbb{K}_i^z \end{array} \right],$$

and

$$\overline{\mathbf{H}}_i = \left(\begin{array}{c} \overline{\mathbf{H}}_i^x \\ \overline{\mathbf{H}}_i^y \\ \overline{\mathbf{H}}_i^z \end{array} \right) = \left(\begin{array}{c} (H_{il}^x)_{1 \leq l \leq d_i} \\ (H_{il}^y)_{1 \leq l \leq d_i} \\ (H_{il}^z)_{1 \leq l \leq d_i} \end{array} \right).$$

- Flux matrix. For simplicity of the presentation, we assume that the mesh is a conforming mesh (i.e. without hanging nodes). We know that $\mathbf{n} = \mathbf{n}^+ = -\mathbf{n}^-$, therefore, for an interior face we have

$$
\begin{aligned}
F_{ik}^{E_x,1} &\equiv \int_F \frac{1}{\tau_{K_i} + \tau_{K_j}} \left[\tau_{K_i} H_i^{t,y} + \tau_{K_j} H_j^{t,y} + \right. \\
&\qquad\qquad \left. \left(\mathbf{n}^+ \times \mathbf{E}_i^t \right)^y + \left(\mathbf{n}^- \times \mathbf{E}_j^t \right)^y \right] n_z \Phi_{ik} - \\
&\qquad \frac{1}{\tau_{K_i} + \tau_{K_j}} \left[\tau_{K_i} H_i^{t,z} + \tau_{K_j} H_j^{t,z} + \right. \\
&\qquad\qquad \left. \left(\mathbf{n}^+ \times \mathbf{E}_i^t \right)^z + \left(\mathbf{n}^- \times \mathbf{E}_j^t \right)^z \right] n_y \Phi_{ik} \\
&= \int_F \frac{1}{\tau_{K_i} + \tau_{K_j}} \left[\left(\sum_{l=1}^{d_i} \tau_{K_i} H_{il}^{t,y} \Phi_{il} + \sum_{m=1}^{d_j} \tau_{K_j} H_{jm}^{t,y} \Phi_{jm} \right) + \right. \\
&\qquad\qquad \left(n_z^+ \sum_{l=1}^{d_i} E_{il}^{t,x} \Phi_{il} - n_x^+ \sum_{l=1}^{d_i} E_{il}^{t,z} \Phi_{il} \right) + \\
&\qquad\qquad \left. \left(n_z^- \sum_{m=1}^{d_j} E_{jm}^{t,x} \Phi_{jm} - n_x^- \sum_{m=1}^{d_j} E_{jm}^{t,z} \Phi_{jm} \right) \right] n_z \Phi_{ik} - \\
&\qquad \frac{1}{\tau_{K_i} + \tau_{K_j}} \left[\left(\sum_{l=1}^{d_i} \tau_{K_i} H_{il}^{t,z} \Phi_{il} + \sum_{m=1}^{d_j} \tau_{K_j} H_{jm}^{t,z} \Phi_{jm} \right) + \right. \\
&\qquad\qquad \left(n_x^+ \sum_{l=1}^{d_i} E_{il}^{t,y} \Phi_{il} - n_y^+ \sum_{l=1}^{d_i} E_{il}^{t,x} \Phi_{il} \right) + \\
&\qquad\qquad \left. \left(n_x^- \sum_{m=1}^{d_j} E_{jm}^{t,y} \Phi_{jm} - n_y^- \sum_{m=1}^{d_j} E_{jm}^{t,x} \Phi_{jm} \right) \right] n_y \Phi_{ik}
\end{aligned}
$$

38

$$= \frac{1}{\tau_{K_i} + \tau_{K_j}} \left[n_z \sum_{l=1}^{d_i} \left(\tau_{K_i} H_{il}^{t,y} + n_z^+ E_{il}^{t,x} - n_x^+ E_{il}^{t,z} \right) \int_F \Phi_{il} \Phi_{ik} + \right.$$

$$n_z \sum_{m=1}^{d_j} \left(\tau_{K_j} H_{jm}^{t,y} + n_z^- E_{jm}^{t,x} - n_x^- E_{jm}^{t,z} \right) \int_F \Phi_{jm} \Phi_{ik} +$$

$$n_y \sum_{l=1}^{d_i} \left(-\tau_{K_i} H_{il}^{t,z} - n_x^+ E_{il}^{t,y} + n_y^+ E_{il}^{t,x} \right) \int_F \Phi_{il} \Phi_{ik} +$$

$$\left. n_y \sum_{m=1}^{d_j} \left(-\tau_{K_j} H_{jm}^{t,z} - n_x^- E_{jm}^{t,y} + n_y^- E_{jm}^{t,x} \right) \int_F \Phi_{jm} \Phi_{ik} \right]$$

$$F_{ik}^{E_x,1} = \frac{1}{\tau_{K_i} + \tau_{K_j}} \left[\sum_{l=1}^{d_i} \tau_{K_i} \left(n_z H_{il}^{t,y} - n_y H_{il}^{t,z} \right) \int_F \Phi_{il} \Phi_{ik} + \right.$$

$$\sum_{m=1}^{d_j} \tau_{K_j} \left(n_z H_{jm}^{t,y} - n_y H_{jm}^{t,z} \right) \int_F \Phi_{jm} \Phi_{ik} +$$

$$\underbrace{\left(n_z^{+2} + n_y^{+2} \right)}_{\left(1 - n_x^{+2} \right)} \left(\sum_{l=1}^{d_i} E_{il}^{t,x} \int_F \Phi_{il} \Phi_{ik} - \sum_{m=1}^{d_j} E_{jm}^{t,x} \int_F \Phi_{jm} \Phi_{ik} \right) +$$

$$n_x^+ n_z^+ \left(\sum_{m=1}^{d_j} E_{jm}^{t,z} \int_F \Phi_{jm} \Phi_{ik} - \sum_{l=1}^{d_i} E_{il}^{t,z} \int_F \Phi_{il} \Phi_{ik} \right) +$$

$$\left. n_x^+ n_y^+ \left(\sum_{m=1}^{d_j} E_{jm}^{t,y} \int_F \Phi_{jm} \Phi_{ik} - \sum_{l=1}^{d_i} E_{il}^{t,y} \int_F \Phi_{il} \Phi_{ik} \right) \right].$$

that is

$$F_{ik}^{E_x,1} = \frac{1}{\tau_{K_i} + \tau_{K_j}} \left[\sum_{l=1}^{d_i} \tau_{K_i} \left(\mathbf{H}_{il}^t \times \mathbf{n} \right)^x \int_F \Phi_{il} \Phi_{ik} + \right.$$

$$\sum_{m=1}^{d_j} \tau_{K_j} \left(\mathbf{H}_{jm}^t \times \mathbf{n} \right)^x \int_F \Phi_{jm} \Phi_{ik} +$$

$$\left. \sum_{m=1}^{d_j} \mathbf{V}_F^x \cdot \mathbf{E}_{jm}^t \int_F \Phi_{jm} \Phi_{ik} - \sum_{l=1}^{d_i} \mathbf{V}_F^x \cdot \mathbf{E}_{il}^t \int_F \Phi_{il} \Phi_{ik} \right].$$

if we further assume that the interpolation degree is the same for each element K_i, i.e. $d_i = d_j = d$, then $\int_F \Phi_{il}\Phi_{ik} = \int_F \Phi_{jm}\Phi_{ik}$ and we get

$$F_{ik}^{E_x,1} = \frac{1}{\tau_{K_i} + \tau_{K_j}} \left(\mathbb{S}_{F,i}\mathbf{V}^{1,i,x}\right)_k, \quad 1 \le k \le d,$$

where

$$\mathbf{V}_F^x = \begin{pmatrix} n_x^2 - 1 \\ n_x n_y \\ n_x n_z \end{pmatrix}, \quad \mathbb{S}_{F,i} = \left(\int_F \Phi_{il}\Phi_{ik}\right)_{1 \le l,k \le d}$$

and

$$\mathbf{V}^{1,i,x} = \left(\tau_{K_i}\left(\mathbf{H}_{il}^t \times \mathbf{n}\right)^x + \tau_{K_j}\left(\mathbf{H}_{jl}^t \times \mathbf{n}\right)^x + \mathbf{V}_F^x \cdot \left(\mathbf{E}_{jl}^t - \mathbf{E}_{il}^t\right)\right)_{1 \le l \le d},$$

where we have introduced the vectors

$$\mathbf{E}_{il} = \begin{pmatrix} E_{il}^x \\ E_{il}^y \\ E_{il}^z \end{pmatrix} \quad \text{and} \quad \mathbf{H}_{il} = \begin{pmatrix} H_{il}^x \\ H_{il}^y \\ H_{il}^z \end{pmatrix}.$$

Proceeding similarly for the last two terms of (27), we obatin

$$F_{ik}^{E_x,2} = \frac{1}{\tau_{K_i}}\left(\mathbb{S}_{F,i}\mathbf{V}^{2,i,x}\right)_k, F_{ik}^{E_x,3} = \frac{1}{\tau_{K_i}+1}\mathbb{S}_{F,i}\left(\mathbf{V}^{2,i,x} + \left(\mathbf{n} \times \mathbf{g}_i^{inc}\right)^x\right)_k, \quad 1 \le k \le d,$$

where

$$\mathbf{V}^{2,i,x} = \left(\tau_{K_i}\left(\mathbf{H}_{il}^t \times \mathbf{n}\right)^x - \mathbf{V}_F^x \cdot \mathbf{E}_{il}^t\right)_{1 \le l \le d},$$

and

$$\left(\mathbf{n} \times \mathbf{g}_i^{inc}\right)^x = \left(\left(\mathbf{n} \times \mathbf{g}_{il}^{inc}\right)^x\right)_{1 \le l \le d}$$

Now, by setting $\mathbf{v} = \boldsymbol{\Phi}^x_{ik} = \begin{pmatrix} \Phi_{ik} \\ 0 \\ 0 \end{pmatrix}$ for $1 \le k \le d$ the equation for H^x_i in (26) becomes

$$\int\limits_{K_i} \mu_i \partial_t H^x_i \Phi_{ik} + \int\limits_{K_i} (E^y_i \partial_z \Phi_{ik} - E^z_i \partial_y \Phi_{ik}) \ -$$

$$\sum_{F \in \partial K_i \cap \mathcal{F}^I_h} \int\limits_F \frac{\tau_{K_i} \tau_{K_j}}{\tau_{K_i} + \tau_{K_j}} \left[\frac{E^{t,y}_i}{\tau_{K_i}} + \frac{E^{t,y}_j}{\tau_{K_j}} - \right.$$

$$\left. \left(\mathbf{n}^+ \times \mathbf{H}^t_i \right)^y - \left(\mathbf{n}^- \times \mathbf{H}^t_j \right)^y \right] n_z \Phi_{ik} \ -$$

$$\frac{\tau_{K_i} \tau_{K_j}}{\tau_{K_i} + \tau_{K_j}} \left[\frac{E^{t,z}_i}{\tau_{K_i}} + \frac{E^{t,z}_j}{\tau_{K_j}} - \right.$$

$$\left. \left(\mathbf{n}^+ \times \mathbf{H}^t_i \right)^z + \left(\mathbf{n}^- \times \mathbf{H}^t_j \right)^z \right] n_y \Phi_{ik} \ -$$

$$\sum_{F \in \partial K_i \cap \Gamma_a} \int\limits_F \frac{1}{\tau_{K_i} + 1} \left[\left(E^{t,y}_i - \tau_{K_i} \left(\mathbf{n} \times \mathbf{H}^t_i \right)^y - \tau_{K_i} \left(\mathbf{n} \times \mathbf{g}^{inc} \right)^y \right) n_z \Phi_{ik} - \right.$$

$$\left. \frac{1}{\tau_{K_i} + 1} \left(E^{t,z}_i - \tau_{K_i} \left(\mathbf{n} \times \mathbf{H}^t_i \right)^z - \tau_{K_i} \left(\mathbf{n} \times \mathbf{g}^{inc} \right)^z \right) n_y \Phi_{ik} \right] = 0.$$
(30)

Developing the different terms in (30) with obtain similar expressions. In particular for the boundary terms, we have

$$F^{H_x,1}_{ik} = \frac{\tau_{K_i} \tau_{K_j}}{\tau_{K_i} + \tau_{K_j}} \left(\mathbb{S}_{F,i} \mathbf{V}^{3,i,x} \right)_k, \quad 1 \le k \le n_d,$$

where

$$\mathbf{V}^{3,i,x} = \left(\frac{1}{\tau_{K_i}} \left(\mathbf{E}^t_{il} \times \mathbf{n} \right)^x + \frac{1}{\tau_{K_j}} \left(\mathbf{E}^t_{jl} \times \mathbf{n} \right)^x + \mathbf{V}^x_F \cdot \left(\mathbf{H}^t_{il} - \mathbf{H}^t_{jl} \right) \right)_{1 \le l \le d},$$

and

$$F^{H_x,2}_{ik} = \frac{\tau_{K_i}}{\tau_{K_i} + 1} \mathbb{S}_{F,i} \left(\mathbf{V}^{4,i,x} + \mathbf{V}^x_F \cdot \mathbf{g}^{inc}_i \right)_k, \quad 1 \le k \le d,$$

where

$$\mathbf{V}^{4,i,x} = \left(\frac{1}{\tau_{K_i}} \left(\mathbf{E}^t_{il} \times \mathbf{n} \right)^x + \mathbf{V}^x_F \cdot \mathbf{H}^t_{il} \right)_{1 \le l \le d}.$$

41

and
$$\mathbf{V}_F^x \cdot \mathbf{g}_i^{inc} = \left(\mathbf{V}_F^x \cdot \mathbf{g}_{il}^{inc}\right)_{1 \leq l \leq d}$$

We can easily see that if $\mathbf{E}_{il}^t = \mathbf{H}_{il}^t = 0$, $\mathbf{E}_{jl} = \mathbf{E}_{jl}^{inc}$ and $\mathbf{H}_{jl} = \mathbf{H}_{jl}^{inc}$ we have

$$\left(\mathbf{n} \times \mathbf{g}_i^{inc}\right)^x = \mathbf{V}^{1,i,x} \quad \text{and} \quad \mathbf{V}_F^x \cdot \mathbf{g}_i^{inc} = \mathbf{V}^{2,i,x}$$

So for a given K_i and for $\mathbf{v} = \mathbf{\Phi}_{ik}^x$, $\ 1 \leq k \leq d$ we have

$$\begin{cases} \varepsilon_i \left(\mathbb{M}_i \partial_t \overline{\mathbf{E}}_i^x\right) & + & \left(\overline{\mathbb{K}}_i \times \overline{\mathbf{H}}_i\right)^x + \displaystyle\sum_{F \in \partial K_i \cap \mathcal{F}_h^I} \frac{1}{\tau_{K_i} + \tau_{K_j}} \mathbb{S}_{F,i} \mathbf{V}^{1,i,x} \\ \\ & + & \displaystyle\sum_{F \in \partial K_i \cap \Gamma_m} \frac{1}{\tau_{K_i}} \left(\mathbb{S}_{F,i} \mathbf{V}^{2,i,x}\right) \\ \\ & + & \displaystyle\sum_{F \in \partial K_i \cap \Gamma_a} \frac{1}{\tau_{K_i} + 1} \mathbb{S}_{F,i} \left(\mathbf{V}^{2,i,x} + \left(\mathbf{n} \times \mathbf{g}_i^{inc}\right)^x\right) = 0, \\ \\ \mu_i \left(\mathbb{M}_i \partial_t \overline{\mathbf{H}}_i^x\right) & - & \left(\overline{\mathbb{K}}_i \times \overline{\mathbf{E}}_i\right)^x - \displaystyle\sum_{F \in \partial K_i \cap \mathcal{F}_h^I} \frac{\tau_{K_i} \tau_{K_j}}{\tau_{K_i} + \tau_{K_j}} \mathbb{S}_{F,i} \mathbf{V}^{3,i,x} \\ \\ & - & \displaystyle\sum_{F \in \partial K_i \cap \Gamma_a} \frac{\tau_{K_i}}{\tau_{K_i} + 1} \mathbb{S}_{F,i} \left(\mathbf{V}^{4,i,x} + \mathbf{V}_F^x \cdot \mathbf{g}_i^{inc}\right) = 0. \end{cases}$$

$$(31)$$

By doing the same calculations with $\mathbf{v} = \mathbf{\Phi}_{ik}^y = \begin{pmatrix} 0 \\ \Phi_{ik} \\ 0 \end{pmatrix}$

and $\mathbf{v} = \mathbf{\Phi}_{ik}^z = \begin{pmatrix} 0 \\ 0 \\ \Phi_{ik} \end{pmatrix}$ for a fixed K_i we obtain for the first system of

42

equations of (31)

$$
\varepsilon_i \begin{pmatrix} \mathbb{M}_i & 0_{d\times d} & 0_{d\times d} \\ 0_{d\times d} & \mathbb{M}_i & 0_{d\times d} \\ 0_{d\times d} & 0_{d\times d} & \mathbb{M}_i \end{pmatrix} \begin{pmatrix} \partial_t \overline{\mathbf{E}}_i^x \\ \partial_t \overline{\mathbf{E}}_i^y \\ \partial_t \overline{\mathbf{E}}_i^z \end{pmatrix} + \begin{pmatrix} \left(\overline{\mathbb{K}}_i \times \overline{\mathbf{H}}_i\right)^x \\ \left(\overline{\mathbb{K}}_i \times \overline{\mathbf{H}}_i\right)^y \\ \left(\overline{\mathbb{K}}_i \times \overline{\mathbf{H}}_i\right)^z \end{pmatrix}
$$

$$
+ \sum_{F\in\partial K_i\cap\mathcal{F}_h^I} \frac{1}{\tau_{K_i}+\tau_{K_j}} \begin{pmatrix} \mathbb{S}_{F,i} & 0_{d\times d} & 0_{d\times d} \\ 0_{d\times d} & \mathbb{S}_{F,i} & 0_{d\times d} \\ 0_{d\times d} & 0_{d\times d} & \mathbb{S}_{F,i} \end{pmatrix} \begin{pmatrix} \mathbf{V}^{1,i,x} \\ \mathbf{V}^{1,i,y} \\ \mathbf{V}^{1,i,z} \end{pmatrix}
$$

$$
+ \sum_{F\in\partial K_i\cap\Gamma_m} \frac{1}{\tau_{K_i}} \begin{pmatrix} \mathbb{S}_{F,i} & 0_{d\times d} & 0_{d\times d} \\ 0_{d\times d} & \mathbb{S}_{F,i} & 0_{d\times d} \\ 0_{d\times d} & 0_{d\times d} & \mathbb{S}_{F,i} \end{pmatrix} \begin{pmatrix} \mathbf{V}^{2,i,x} \\ \mathbf{V}^{2,i,y} \\ \mathbf{V}^{2,i,z} \end{pmatrix} \qquad (32)
$$

$$
+ \sum_{F\in\partial K_i\cap\Gamma_a} \frac{1}{\tau_{K_i}+1} \begin{pmatrix} \mathbb{S}_{F,i} & 0_{d\times d} & 0_{d\times d} \\ 0_{d\times d} & \mathbb{S}_{F,i} & 0_{d\times d} \\ 0_{d\times d} & 0_{d\times d} & \mathbb{S}_{F,i} \end{pmatrix} \begin{pmatrix} \mathbf{V}^{2,i,x} \\ \mathbf{V}^{2,i,y} \\ \mathbf{V}^{2,i,z} \end{pmatrix}
$$

$$
+ \frac{1}{\tau_{K_i}+1} \begin{pmatrix} \mathbb{S}_{F,i} & 0_{d\times d} & 0_{d\times d} \\ 0_{d\times d} & \mathbb{S}_{F,i} & 0_{d\times d} \\ 0_{d\times d} & 0_{d\times d} & \mathbb{S}_{F,i} \end{pmatrix} \begin{pmatrix} \left(\mathbf{n}\times\mathbf{g}_i^{inc}\right)^x \\ \left(\mathbf{n}\times\mathbf{g}_i^{inc}\right)^y \\ \left(\mathbf{n}\times\mathbf{g}_i^{inc}\right)^z \end{pmatrix} = 0,
$$

and

$$
\mu_i \begin{pmatrix} \mathbb{M}_i & 0_{d\times d} & 0_{d\times d} \\ 0_{d\times d} & \mathbb{M}_i & 0_{d\times d} \\ 0_{d\times d} & 0_{d\times d} & \mathbb{M}_i \end{pmatrix} \begin{pmatrix} \partial_t \overline{\mathbf{H}}_i^x \\ \partial_t \overline{\mathbf{H}}_i^y \\ \partial_t \overline{\mathbf{H}}_i^z \end{pmatrix} - \begin{pmatrix} \left(\overline{\mathbb{K}}_i \times \overline{\mathbf{E}}_i\right)^x \\ \left(\overline{\mathbb{K}}_i \times \overline{\mathbf{E}}_i\right)^y \\ \left(\overline{\mathbb{K}}_i \times \overline{\mathbf{E}}_i\right)^z \end{pmatrix}
$$

$$
- \sum_{F\in\partial K_i\cap\mathcal{F}_h^I} \frac{\tau_{K_i}\tau_{K_j}}{\tau_{K_i}+\tau_{K_j}} \begin{pmatrix} \mathbb{S}_{F,i} & 0_{d\times d} & 0_{d\times d} \\ 0_{d\times d} & \mathbb{S}_{F,i} & 0_{d\times d} \\ 0_{d\times d} & 0_{d\times d} & \mathbb{S}_{F,i} \end{pmatrix} \begin{pmatrix} \mathbf{V}^{3,i,x} \\ \mathbf{V}^{3,i,y} \\ \mathbf{V}^{3,i,z} \end{pmatrix} \qquad (33)
$$

$$
- \sum_{F\in\partial K_i\cap\Gamma_a} \frac{1}{\tau_{K_i}+1} \begin{pmatrix} \mathbb{S}_{F,i} & 0_{d\times d} & 0_{d\times d} \\ 0_{d\times d} & \mathbb{S}_{F,i} & 0_{d\times d} \\ 0_{d\times d} & 0_{d\times d} & \mathbb{S}_{F,i} \end{pmatrix} \begin{pmatrix} \mathbf{V}^{4,i,x} \\ \mathbf{V}^{4,i,y} \\ \mathbf{V}^{4,i,z} \end{pmatrix}
$$

$$
+ \frac{\tau_{K_i}}{\tau_{K_i}+1} \begin{pmatrix} \mathbb{S}_{F,i} & 0_{d\times d} & 0_{d\times d} \\ 0_{d\times d} & \mathbb{S}_{F,i} & 0_{d\times d} \\ 0_{d\times d} & 0_{d\times d} & \mathbb{S}_{F,i} \end{pmatrix} \begin{pmatrix} \mathbf{V}_F^x \cdot \mathbf{g}_i^{inc} \\ \mathbf{V}_F^y \cdot \mathbf{g}_i^{inc} \\ \mathbf{V}_F^z \cdot \mathbf{g}_i^{inc} \end{pmatrix} = 0.
$$

Where :

$$
\mathbf{V}_F^y = \begin{pmatrix} n_y n_x \\ n_y^2 - 1 \\ n_y n_z \end{pmatrix}, \mathbf{V}_F^z = \begin{pmatrix} n_z n_x \\ n_z n_y \\ n_z^2 - 1 \end{pmatrix}
$$

So for every K_i we have:

$$
\begin{cases}
\varepsilon_i \left(\overline{\mathbb{M}}_i \partial_t \overline{\mathbf{E}}_i \right) + \left(\overline{\mathbb{K}}_i \times \overline{\mathbf{H}}_i \right) + \sum_{F \in \partial K_i \cap \mathcal{F}_h^I} \frac{1}{\tau_{K_i} + \tau_{K_j}} \overline{\mathbb{S}}_{F,i} \mathbf{V}^{1,i} + \\[2ex]
\sum_{F \in \partial K_i \cap \Gamma_m} \frac{1}{\tau_{K_i}} \left(\overline{\mathbb{S}}_{F,i} \mathbf{V}^{2,i} \right) + \\[2ex]
\sum_{F \in \partial K_i \cap \Gamma_a} \frac{1}{\tau_{K_i} + 1} \overline{\mathbb{S}}_{F,i} \left(\mathbf{V}^{2,i} + \mathbf{n} \times \mathbf{g}^{\mathbf{inc}} \right) = 0, \\[2ex]
\mu_i \left(\overline{\mathbb{M}}_i \partial_t \overline{\mathbf{H}}_i \right) - \left(\overline{\mathbb{K}}_i \times \overline{\mathbf{E}}_i \right) - \sum_{F \in \partial K_i \cap \mathcal{F}_h^I} \frac{\tau_{K_i} \tau_{K_j}}{\tau_{K_i} + \tau_{K_j}} \overline{\mathbb{S}}_{F,i} \mathbf{V}^{3,i} - \\[2ex]
\sum_{F \in \partial K_i \cap \Gamma_a} \frac{1}{\tau_{K_i} + 1} \overline{\mathbb{S}}_{F,i} \left(\mathbf{V}^{4,i} + \tau_{K_i} \mathbf{V}_F^{inc} \right) = 0,
\end{cases}
\tag{34}
$$

where

$$
\mathbf{V}_F^{inc} = \begin{pmatrix} \mathbf{V}_F^x \cdot \mathbf{g}^{inc} \\ \mathbf{V}_F^y \cdot \mathbf{g}^{inc} \\ \mathbf{V}_F^z \cdot \mathbf{g}^{inc} \end{pmatrix}.
$$

References

[1] A. Taflove, S. Hagness, Computational electrodynamics: the finite-difference time-domain method - 3rd ed., Artech House Publishers, 2005.

[2] S. Pernet, X. Ferriéres, G. Cohen, High spatial order finite element method to solve Maxwell's equations in time-domain, IEEE Trans. Ant. and Propag. 53 (9) (2006) 2889–2899.

[3] J. Hesthaven, T. Warburton, Nodal high-order methods on unstructured grids. I. Time-domain solution of Maxwell's equations, J. Comput. Phys. 181 (1) (2002) 186–221.

[4] V. Kabakian, V. Shankar, W. Hall, Unstructured grid-based discontinuous Galerkin method for broadband electromagnetic simulations, J. Sci. Comput. 20 (3) (2004) 405–431.

[5] M. Chen, B. Cockburn, F. Reitich, High-order RKDG methods for computational electromagnetics, J. Sci. Comput. 22-23 (2005) 205–226.

[6] B. Cockburn, F. Li, C.-W. Shu, Locally divergence-free discontinuous Galerkin methods for the Maxwell equations, J. Comp. Phys. 194 (2) (2004) 588–610.

[7] L. Fezoui, S. Lanteri, S. Lohrengel, S. Piperno, Convergence and stability of a discontinuous Galerkin time-domain method for the 3D heterogeneous Maxwell equations on unstructured meshes, ESAIM: Math. Model. Numer. Anal. 39 (6) (2005) 1149–1176.

[8] G. Cohen, X. Ferriéres, S. Pernet, A spatial high order hexahedral discontinuous Galerkin method to solve Maxwell's equations in time-domain, J. Comput. Phys. 217 (2) (2006) 340–363.

[9] S. Dosopoulos, J. Lee, Interconnect and lumped elements modeling in interior penalty discontinuous Galerkin time-domain methods, J. Comput. Phys. 229 (2) (2010) 8521–8536.

[10] S. Dosopoulos, J. Lee, Interior penalty discontinuous Galerkin finite element method for the time-dependent first order Maxwell's equations, IEEE Trans. Ant. and Propag. 58 (12) (2010) 4085–4090.

[11] J. Alvarez, L. Angulo, A. Bretones, S. Garcia, A spurious-free discontinuous Galerkin time-domain method for the accurate modeling of microwave filters, IEEE Trans. Microw. Theory Tech. 60 (8) (2012) 2359–2369.

[12] J. Alvarez, L. Angulo, A. Bretones, S. Garcia, 3-D discontinuous Galerkin time-domain method for anisotropic materials, IEEE Ant. Wir. Prop. Lett. 11 (2012) 1182–1185.

[13] B. Z. S. Dosopoulos, J. F. Lee, Non-conformal and parallel discontinuous Galerkin time domain method for Maxwell's equations: EM analysis of IC packages, J. Comput. Phys. 238 (1) (2013) 48–70.

[14] P. Li, L. Jiang, H. Bagci, Cosimulation of electromagnetics-circuit systems exploiting DGTD and MNA, IEEE Trans. Compon. Pack. Manuf. Tech. 4 (6) (2014) 1052–1061.

[15] R. Diehl, K. Busch, J. Niegemann, Comparison of low-storage Runge-Kutta schemes for discontinuous Galerkin time-domain simulations of Maxwell's equations, J. Comp. Theor. Nanosc. 7 (2010) 1572.

[16] S. G. A.Hille, R. Kullock, L. M. Eng, Improving nano-optical simulations through curved elements implemented within the discontinuous Galerkin method computational, J. Comp. Theor. Nanosc. 7 (2010) 1581–1586.

[17] M. König, K. Busch, J. Niegemann, The Discontinuous Galerkin Time-Domain method for Maxwell's equations with anisotropic materials, Photonics and Nanostructures - Fundamentals and Applications 8 (4) (2010) 303–309.

[18] K. Busch, M. König, J. Niegemann, Discontinuous Galerkin methods in nanophotonics, Laser and Photonics Reviews 5 (2011) 1–37.

[19] H. Songoro, M. Vogel, Z. Cendes, Keeping time with Maxwell's equations, IEEE Microw. 11 (2) (2010) 42–49.

[20] J. Diaz, M. Grote, Energy conserving explicit local time-stepping for second-order wave equations, SIAM J. Sci. Comput. 31 (2009) 1985–2014.

[21] M. Grote, M. Mehlin, T. Mitkova, Runge-Kutta-based explicit local time-stepping methods for wave propagation, SIAM J. Sci. Comput. 37 (A774-A775) (2015) 2.

[22] S. Piperno, Symplectic local time stepping in non-dissipative DGTD methods applied to wave propagation problem, ESAIM: Math. Model. Num. Anal. 40 (5) (2006) 815–841.

[23] M. Grote, T. Mitkova, Explicit local time-stepping methods for Maxwel's equations, J. Comp. Appl. Math. 234 (3283–3302) (2010) 12.

[24] A. Taube, M. Dumbser, C. Munz, R. Schneider, A high-order discontinuous Galerkin method with time-accurate local time stepping for the Maxwell equations, Int. J. Numer. Model. 22 (2009) 77–103.

[25] L. Moya, Temporal convergence of a locally implicit discontinuous Galerkin method for Maxwell's equations, ESAIM Math. Model. Numer. Anal. (M2AN) 46 (2012) 1225–1246.

[26] L. Moya, S. Descombes, S. Lanteri, Locally implicit time integration strategies in a discontinuous Galerkin method for Maxwell's equations, J. Sci. Comp. 56 (1) (2013) 190–218.

[27] B. Cockburn, J. Gopalakrishnan, R. Lazarov, Unified hybridization of discontinuous Galerkin, mixed, and continuous Galerkin methods for second order elliptic problems, SIAM J. Numer. Anal. 47 (2) (2009) 1319–1365.

[28] N. Nguyen, J. Peraire, Hybridizable discontinuous Galerkin methods for partial differential equations in continuum mechanics, J. Comput. Phys. 231 (18) (2012) 5955–5988.

[29] N. Nguyen, J. Peraire, B. Cockburn, Hybridizable discontinuous Galerkin methods for the time-harmonic Maxwell's equations, J. Comput. Phys. 230 (19) (2011) 7151–7175.

[30] L. Li, S. Lanteri, R. Perrussel, Numerical investigation of a high order hybridizable discontinuous Galerkin method for 2d time-harmonic Maxwell's equations, COMPEL 2 (3) (2013) 1112–1138.

[31] L. Li, S. Lanteri, R. Perrussel, A hybridizable discontinuous Galerkin method combined to a Schwarz algorithm for the solution of 3d time-harmonic Maxwell's equations, J. Comput. Phys. 256 (2014) 563–581.

[32] M. Kronbichler, S. Schoeder, C. Müller, W. Wall, Comparison of implicit and explicit hybridizable discontinuous Galerkin methods for the acoustic wave equation, Int. J. Num. Meth. Engrg.

[33] M. Stanglmeier, N. Nguyen, J. Peraire, B. Cockburn, An explicit hybridizable discontinuous Galerkin method for the acoustic wave equation, Comput. Meth. App. Mech. Engrg. 300 (2016) 748–769.

[34] M. Carpenter, C. Kennedy, Fourth-order 2N-storage Runge-Kutta schemes, Tech. Rep. 109112, NASA (1994).

[35] H. Duan, P. Lin, R. C.E.Tan, Analysis of a continuous finite element method for h(curl;div)-elliptic interface problem, Numer. Math. (2013) 12.

[36] J. Williamson, Low-storage Runge-Kutta schemes, J. Comput. Phys. 35 (1980) 48–56.

[37] Abgrall, Rémi, Shu, Chi-Wang (Eds.), Handbook of numerical methods for hyperbolic problems, Vol. 17, Elsevier/North-Holland, Amsterdam, 2016.